

Articles	
1549-1560	<a href="#">In vitro and in vivo characterization of <i>Clostridium scindens</i> bile acid transformations</a>
1561-1570	<a href="#">The gut microbiome in health and disease</a>
1571-1580	<a href="#">The gut microbiome in health and disease</a>
1581-1590	<a href="#">The gut microbiome in health and disease</a>
1591-1600	<a href="#">The gut microbiome in health and disease</a>
1601-1610	<a href="#">The gut microbiome in health and disease</a>
1611-1620	<a href="#">The gut microbiome in health and disease</a>
1621-1630	<a href="#">The gut microbiome in health and disease</a>
1631-1640	<a href="#">The gut microbiome in health and disease</a>
1641-1650	<a href="#">The gut microbiome in health and disease</a>
1651-1660	<a href="#">The gut microbiome in health and disease</a>
1661-1670	<a href="#">The gut microbiome in health and disease</a>
1671-1680	<a href="#">The gut microbiome in health and disease</a>
1681-1690	<a href="#">The gut microbiome in health and disease</a>
1691-1700	<a href="#">The gut microbiome in health and disease</a>
1701-1710	<a href="#">The gut microbiome in health and disease</a>
1711-1720	<a href="#">The gut microbiome in health and disease</a>
1721-1730	<a href="#">The gut microbiome in health and disease</a>
1731-1740	<a href="#">The gut microbiome in health and disease</a>
1741-1750	<a href="#">The gut microbiome in health and disease</a>
1751-1760	<a href="#">The gut microbiome in health and disease</a>
1761-1770	<a href="#">The gut microbiome in health and disease</a>
1771-1780	<a href="#">The gut microbiome in health and disease</a>
1781-1790	<a href="#">The gut microbiome in health and disease</a>
1791-1800	<a href="#">The gut microbiome in health and disease</a>
1801-1810	<a href="#">The gut microbiome in health and disease</a>
1811-1820	<a href="#">The gut microbiome in health and disease</a>
1821-1830	<a href="#">The gut microbiome in health and disease</a>
1831-1840	<a href="#">The gut microbiome in health and disease</a>
1841-1850	<a href="#">The gut microbiome in health and disease</a>
1851-1860	<a href="#">The gut microbiome in health and disease</a>
1861-1870	<a href="#">The gut microbiome in health and disease</a>
1871-1880	<a href="#">The gut microbiome in health and disease</a>
1881-1890	<a href="#">The gut microbiome in health and disease</a>
1891-1900	<a href="#">The gut microbiome in health and disease</a>
1901-1910	<a href="#">The gut microbiome in health and disease</a>
1911-1920	<a href="#">The gut microbiome in health and disease</a>
1921-1930	<a href="#">The gut microbiome in health and disease</a>
1931-1940	<a href="#">The gut microbiome in health and disease</a>
1941-1950	<a href="#">The gut microbiome in health and disease</a>
1951-1960	<a href="#">The gut microbiome in health and disease</a>
1961-1970	<a href="#">The gut microbiome in health and disease</a>
1971-1980	<a href="#">The gut microbiome in health and disease</a>
1981-1990	<a href="#">The gut microbiome in health and disease</a>
1991-2000	<a href="#">The gut microbiome in health and disease</a>

## *In vitro* and *in vivo* characterization of *Clostridium scindens* bile acid transformations

Solenne Marion, Nicolas Studer, Lyne Desharnais, Laure Menin, Stéphane Escrig, Anders Meibom, Siegfried Hapfelmeier & Rizlan Bernier-Latmani

To cite this article: Solenne Marion, Nicolas Studer, Lyne Desharnais, Laure Menin, Stéphane Escrig, Anders Meibom, Siegfried Hapfelmeier & Rizlan Bernier-Latmani (2018): *In vitro* and *in vivo* characterization of *Clostridium scindens* bile acid transformations, Gut Microbes, DOI: 10.1080/19490976.2018.1549420

To link to this article: <https://doi.org/10.1080/19490976.2018.1549420>



© 2018 The Author(s). Published with license by Taylor & Francis Group, LLC



View supplementary material



Published online: 27 Dec 2018.



Submit your article to this journal



Article views: 245








View Crossmark data

RESEARCH PAPER



## *In vitro* and *in vivo* characterization of *Clostridium scindens* bile acid transformations

Solenne Marion<sup>a</sup>, Nicolas Studer <sup>b</sup>, Lyne Desharnais<sup>a</sup>, Laure Menin<sup>c</sup>, Stéphane Escrig <sup>d</sup>, Anders Meibom <sup>d,e</sup>, Siegfried Hapfelmeier <sup>b</sup>, and Rizlan Bernier-Latmani <sup>a</sup>

<sup>a</sup>Environmental Microbiology Laboratory, École Polytechnique Fédérale de Lausanne (EPFL), Lausanne, Switzerland; <sup>b</sup>Institute for Infectious Diseases, University of Bern, Bern, Switzerland; <sup>c</sup>Institute of Chemical Sciences and Engineering, École Polytechnique Fédérale de Lausanne (EPFL), Lausanne, Switzerland; <sup>d</sup>Laboratory for Biological Geochemistry, École Polytechnique Fédérale de Lausanne (EPFL), Lausanne, Switzerland; <sup>e</sup>Center for Advanced Surface Analysis, Université de Lausanne, Lausanne, Switzerland

### ABSTRACT

The human gut hosts trillions of microorganisms that exert a profound influence on human biology. Gut bacteria communicate with their host by secreting small molecules that can signal to distant organs in the body. Bile acids are one class of these signaling molecules, synthesized by the host and chemically transformed by the gut microbiota. Among bile acid metabolizers, bile acid 7-dehydroxylating bacteria are commensals of particular importance as they carry out the 7-dehydroxylation of liver-derived primary bile acids to 7-dehydroxylated bile acids. The latter represents a major fraction of the secondary bile acid pool. The microbiology of this group of gut microorganisms is understudied and warrants more attention. Here, we detail the bile acid transformations carried out by the 7-dehydroxylating bacterium *Clostridium scindens* *in vitro* and *in vivo*. *In vitro*, *C. scindens* exhibits not only 7 $\alpha$ -dehydroxylating capabilities but also, the ability to oxidize other hydroxyl groups and reduce ketone groups in primary and secondary bile acids. This study revealed 12-oxolithocholic acid as a major transient product in the 7 $\alpha$ -dehydroxylation of cholic acid. Furthermore, the *in vivo* study included complementing a gnotobiotic mouse line (devoid of the ability to 7-dehydroxylate bile acids) with *C. scindens* and investigating its colonization dynamics and bile acid transformations. Using NanoSIMS (Nanoscale Secondary Ion Mass Spectrometry), we demonstrate that the large intestine constitutes a niche for *C. scindens*, where it efficiently 7-dehydroxylates cholic acid to deoxycholic acid. Overall, this work reveals a novel transient species during 7-dehydroxylation as well as provides direct evidence for the colonization and growth of 7-dehydroxylating bacteria in the large intestine.

### ARTICLE HISTORY

Received 20 July 2018  
Revised 26 October 2018  
Accepted 13 November 2018

### KEYWORDS



Bile salts; 7 $\alpha$ -dehydroxylation pathway; clostridium; commensal bacteria; intestinal colonization; gut ecology; lithocholic acid (LCA); deoxycholic acid (DCA); 12-oxo bile acids; stable isotopes

## Introduction


Bile acids (BAs) are endogenous molecules synthesized from cholesterol in the liver and stored in the gall bladder. Upon meal stimulation, they are released into the duodenum to facilitate the solubilization and absorption of lipids and lipid-soluble vitamins.<sup>1</sup> A major fraction of the BA pool (> 95%), actively reabsorbed in the terminal ileum and passively along the entire intestinal tract, returns to the liver through the hepatic portal vein. Only a small proportion of the BA pool (5%) enters the large intestine. This cycle is referred to as the enterohepatic circulation of BAs and occurs several times per day. During the

cycle, a small fraction of BAs escapes hepatic uptake and reaches the systemic circulation.

Bile acids act as signaling molecules and are thought to play a key role in the maintenance of the host's health. In addition to their local action in the intestine, they are proposed to reach other organs in the human body (via the systemic circulation).<sup>2</sup> Bile acid receptors are found on many organs and tissues (e.g., liver, pancreas, intestine, brown adipose tissue), as well as on immune cells, suggesting the broad field of action of these compounds.<sup>3</sup> Bile acids also act indirectly when they activate receptors that induce the release of other signaling molecules. For instance, the activation of the BA receptor Takeda G-protein receptor 5 (TGR5) induces Glucagon-Like

**CONTACT** Rizlan Bernier-Latmani  [rizlan.bernier-latmani@epfl.ch](mailto:rizlan.bernier-latmani@epfl.ch)  Environmental Microbiology Laboratory, École Polytechnique Fédérale de Lausanne (EPFL), Lausanne, Switzerland

This article has been republished with minor changes. These changes do not impact the academic content of the article.

 Supplemental data for this article can be accessed on the [publisher's website](#).

© 2018 The Author(s). Published with license by Taylor & Francis Group, LLC

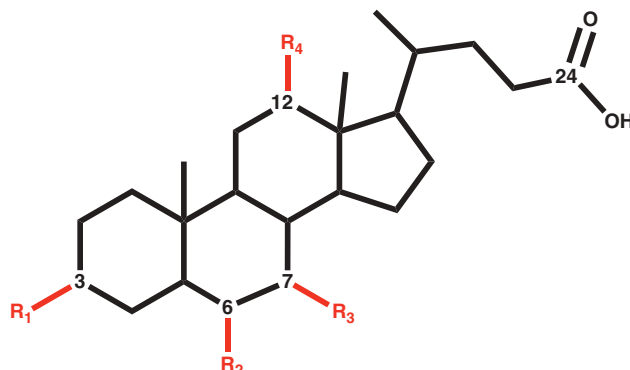
This is an Open Access article distributed under the terms of the Creative Commons Attribution-NonCommercial-NoDerivatives License (<http://creativecommons.org/licenses/by-nc-nd/4.0/>), which permits non-commercial re-use, distribution, and reproduction in any medium, provided the original work is properly cited, and is not altered, transformed, or built upon in any way.

Peptide-1 (GLP-1) production by entero-endocrine L-cells, which subsequently potentiates  $\beta$ -cell glucose-induced insulin secretion in the pancreas.<sup>4</sup>

In the human intestinal tract, the two liver-derived primary BAs (Figure 1), conjugated cholic acid (CA) and chenodeoxycholic acid (CDCA), undergo several transformations mediated by gut microbes, leading to a large diversity of secondary bile acids. The microbial transformation of BAs in the gut is critical to BA-mediated signaling as it modifies their affinity for specific BA receptors.<sup>5</sup> Bile acid 7-dehydroxylating bacteria are a group of gut commensals of particular importance as they catalyze the dehydroxylation of liver-derived (primary) BAs at the C7 position (i.e., 7-dehydroxylation) and produce 7-dehydroxylated BAs, which represent a large

fraction of the secondary BA pool in the large intestine. Bile acids transformed by these bacteria are agonists for TGR5, which is involved in the regulation of metabolism and energy expenditure as well as inflammation.<sup>6</sup> In addition, BAs lacking the 7-hydroxyl group are also associated with protection from infection by a specific intestinal pathogen, *Clostridium difficile*.<sup>7</sup>

The microbial transformations undergone by BAs in the gut play an important role in health<sup>5</sup>, and modulation of the bile acid pool composition represents a promising avenue for the prevention and treatment of various diseases.<sup>8</sup> Perturbation of the bile acid pool is linked to major metabolic diseases (e.g., obesity, type 2 diabetes, non-alcoholic fatty liver disease)<sup>9</sup>, cardiovascular diseases (e.g., atherosclerosis)<sup>9</sup>, inflammatory diseases



Bile Acid Name	Abbreviations	R1	R2	R3	R4	ketone group
Cholic acid	CA	3 $\alpha$		7 $\alpha$	12 $\alpha$	-
Chenodeoxycholic acid	CDCA	3 $\alpha$		7 $\alpha$		-
$\alpha$ -Muricholic acid	$\alpha$ MCA	3 $\alpha$	6 $\beta$	7 $\alpha$		-
$\beta$ -Muricholic acid	$\beta$ MCA	3 $\alpha$	6 $\beta$	7 $\beta$		-
Ursodeoxycholic acid	UDCA	3 $\alpha$		7 $\beta$		-
Deoxycholic acid	DCA	3 $\alpha$			12 $\alpha$	-
Lithocholic acid	LCA	3 $\alpha$				-
3-oxodeoxycholic acid	3-oxoDCA				12 $\alpha$	R1
3-oxocholic acid	3-oxoCA			7 $\alpha$	12 $\alpha$	R1
7-oxodeoxycholic acid	7-oxoDCA	3 $\alpha$			12 $\alpha$	R3
7-oxolithocholic acid	7-oxoLCA	3 $\alpha$				R3
12-oxolithocholic acid	12-oxoLCA	3 $\alpha$				R4

**Figure 1.** Structures of selected human and murine bile acids. Bile acids differ by the position of the hydroxyl groups on the molecule. CA and CDCA are found both in humans and rodents, while UDCA and the muricholic acids are primary BAs synthesized only in rodents. In humans, UDCA is produced from CDCA by microbial enzymes and therefore, is considered as a secondary bile acid. The full list of BAs considered in this study and their structures is included in supplemental information (Table S1).

(e.g., inflammatory bowel disease), gastrointestinal cancers<sup>10</sup>, as well as *Clostridium difficile* infection.<sup>7</sup> Collectively, these diseases exact a heavy socio-economic toll due to their increasing occurrence and severity in first-world countries. Bile acid metabolizing bacteria, particularly 7-dehydroxylating organisms, represent a promising target to modulate the bile acid pool and consequently host physiology.<sup>11</sup> However, much remains to be deciphered about this group of microorganisms, including their metabolism, diversity, abundance in the gut, and colonization dynamics in the host.

The spatial organization of the gut microbial community is suggested to be linked to their function within the host.<sup>12,13</sup> Only one study, conducted by Midvedt and Norman (1968), has explored the distribution of bile acid-metabolizing bacteria along the intestinal tract (in this case in rats).<sup>14</sup> They pointed out that the organisms responsible for the elimination of the 7 $\alpha$ -hydroxyl of bile acids are found in the cecum and feces of rats. Other studies have probed the bile acid composition longitudinally along the intestinal tract and observed the formation of deoxycholic acid (DCA) and lithocholic acid (LCA), the products of 7 $\alpha$ -dehydroxylation of CA and CDCA, respectively, mainly in the cecum and colon<sup>15</sup>, suggesting the large intestine is a colonization site for 7-dehydroxylating bacteria. However, concluding the presence or absence of certain microorganisms only based on the *in vivo* bile acid composition lacks rigor since it does not link specific organisms with their *in vivo* activity. Several studies reported discrepancies in bile acid transformations by bacteria *in vitro* or *in vivo*. For instance, Narushima *et al.* (1999), observed that *Clostridium sp.* TO-931 (now known as *Clostridium hiranonis*<sup>16</sup>) did not deconjugate tauro-conjugated bile acids in germ-free mice, although its ability to deconjugate taurocholic acid (TCA) was shown *in vitro*.<sup>17</sup> Furthermore, side chain conjugation of bile acids precludes 7-dehydroxylation.<sup>18</sup> Thus, if the 7-dehydroxylating bacteria does not synthesize bile salts hydrolases (deconjugating enzymes), they will rely on deconjugating bacteria to perform 7-dehydroxylation. *Clostridium hiranonis* is a known 7 $\alpha$ -dehydroxylating and deconjugating species, but it did not perform deconjugation nor 7 $\alpha$ -dehydroxylation *in vivo* even in the presence of an additional deconjugating strain (*Bacteroides diastonicus* K-5).<sup>17</sup> Bile acid 7 $\alpha$ -dehydroxylation *in vivo* is likely to

be influenced by various factors including pH, oxygen partial pressure<sup>19</sup>, enzymatic co-factors (e.g., flavins)<sup>20</sup>, the bile acid pool, and gut microbes. Examples of intestinal bacteria influencing bile acid 7 $\alpha$ -dehydroxylation include *Bacteroides sp.* and a *Ruminococcus* strain. *Bacteroides sp.* enhances bile acid 7 $\alpha$ -dehydroxylation by *Eubacterium sp.* strain c-25 *via* an unknown mechanism.<sup>21</sup> The *Ruminococcus* strain secretes a soluble factor necessary for the growth of the 7 $\alpha$ -dehydroxylating strain HDCA-1.<sup>22</sup> Hence, the production of 7-dehydroxylated secondary bile acid results from complex interactions between the host, the 7-dehydroxylating species and the gut microbial community.

The model organism used in this study, *Clostridium scindens*, is one of the major 7-dehydroxylating bacteria found in humans<sup>23,24</sup> and rodents.<sup>25</sup> This bacterium was first isolated from feces of a patient with colon cancer and characterized by Holdeman and Moore in 1973.<sup>26</sup> Forty-two years later, *C. scindens* was identified as a potential protective gut commensal against *Clostridium difficile* infection.<sup>7</sup> The 7-dehydroxylated secondary bile acids (e.g., DCA and LCA) produced by bile acid 7-dehydroxylating bacteria impact *C. difficile* spore germination and outgrowth, thus preventing the onset of disease.<sup>27,28</sup>

The objectives of the study are 1) to investigate the bile acids transformations performed by *Clostridium scindens in vitro*, and *in vivo* in a gnotobiotic mouse model, and 2) to explore its colonization dynamics in the murine intestinal tract using Nanoscale Secondary Ion Mass Spectrometry (NanoSIMS).<sup>29</sup> This study provides a better understanding of the microbiology of 7-dehydroxylating organisms, and is motivated by the fact that these commensals constitute a direct link between bile acids and host health.

## Results

### *Clostridium scindens* growth in the presence of human and murine bile acids *in vitro*

OD<sub>600</sub> measurements were used to quantify the growth of *Clostridium scindens* as a function of time and to assess the impact of primary bile acids on the growth of this organism (Figure 2(a)). The primary bile acids CA, UDCA,  $\alpha$ MCA and  $\beta$ MCA

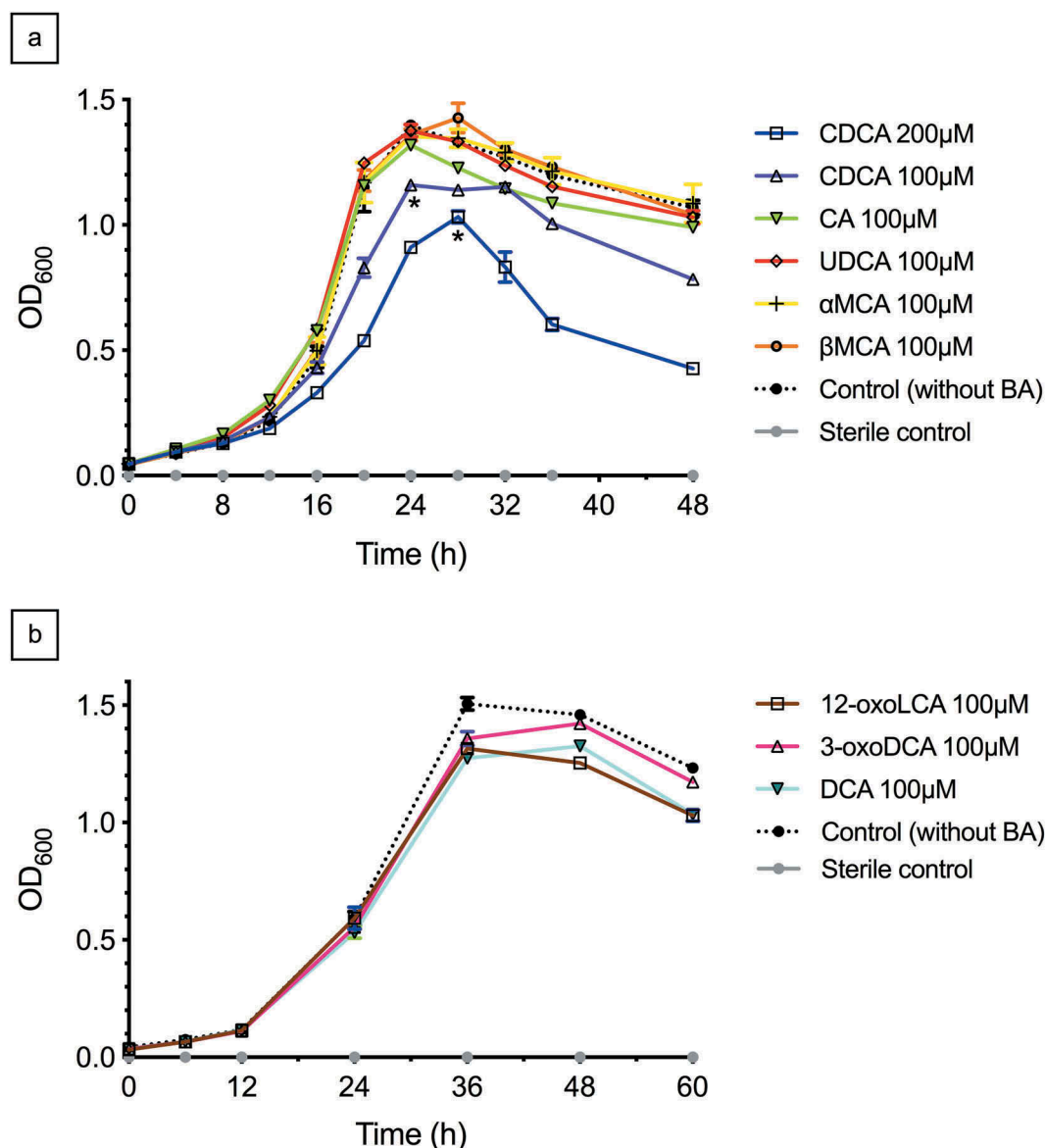


**Figure 2.** Impact of primary and secondary bile acids on *C. scindens* growth. *C. scindens* was grown in BHIS-S medium containing a) one primary bile acid (CA, CDCA, UDCA, αMCA, βMCA) or b) one secondary bile acid (DCA, 3-oxoDCA, 12-oxoLCA). A control without bile acids and one sterile control were prepared in parallel. For each bile acid condition or the controls, cultures were prepared in triplicate. Growth of *C. scindens* was quantified with OD<sub>600</sub> measurements of samples collected from triplicate cultures of *C. scindens*. Each symbol indicates the mean and the standard deviation. Statistical analysis used the Holm-Sidak test to compare the maximal cell density mean of each bile acid condition to the maximal cell density mean of the control without bile acid. The absence of a symbol under the maximal density time point indicates that there was no statistically significant difference ( $p > 0.05$ ) relative to the control group (\* =  $p < 0.05$ ).

had no significant effect on *C. scindens* *in vitro* compared to the control cultures without bile acids. The biomass was maximal after 24 h of incubation in media containing CA (OD<sub>max</sub>  $\approx 1.32 \pm 0.015$ ), UDCA ( $1.38 \pm 0.025$ ), αMCA ( $1.35 \pm 0.015$ ) and after 28 h of incubation in βMCA medium ( $1.43 \pm 0.060$ ). In the absence of bile acids (i.e., the control), a peak cell density of OD<sub>600</sub> =  $1.40 \pm 0.021$  was reached at 24 h of

incubation. Of all the primary bile acids tested, only CDCA had a significant impact on *C. scindens* growth, resulting in a slower growth rate, a reduced peak cell density and a lower end point cell density in a dose-dependent manner. The maximal cell density was reached after 24 h and 28 h of incubation in the media containing CDCA 100μM ( $1.16 \pm 0.016$ ) and CDCA 200μM ( $1.03 \pm 0.023$ ), respectively.



Overall, *C. scindens* is resistant to most primary bile acids *in vitro*. Additionally, we also investigated the impact of selected secondary bile acids (DCA, 12-oxoLCA and 3-oxoDCA) on the growth of *C. scindens*. These compounds did not exhibit any evidence of toxicity at a concentration of 100  $\mu\text{M}$  (Figure 2(b)). Next, we investigated the bile acid transformations performed by *C. scindens* *in vitro*.

### *In vitro* bile acid transformations by *Clostridium scindens*

In order to investigate *C. scindens* bile acid transformations *in vitro*, bile acid analyses were performed on the culture supernatants (representing dissolved BAs (SUP)) and pellets (representing cell-associated BAs (PEL)). Furthermore, in order to discriminate between BAs in the cytoplasm from those bound to the cell envelope, we separated the cytoplasmic and cell envelope fraction of the biomass by ultracentrifugation after cell lysis

for selected pellet samples, and analyzed the bile acids in both fractions.

We observed that *C. scindens* removes the C7-hydroxyl group from CA and CDCA. CA is partially 7 $\alpha$ -dehydroxylated to DCA, as reported previously<sup>30</sup>, and 12-oxoLCA is also produced (Figure 3(a)). Overall, about 83% of the CA is converted to 7-dehydroxylated bile acid species (DCA and 12-oxoLCA) after a 24 h incubation. In contrast, *C. scindens* converted only 10% of CDCA to LCA after 52 h of incubation (Figure 3(d)), presumably partly due to the toxicity of this compound. The major 7-dehydroxylated secondary bile acids of CA include DCA and 12-oxoLCA, and those from CDCA include LCA and 3-oxoLCA. The 3 $\beta$ -epimer of LCA (isoLCA) was also detected (Figures 3(d) and 3(e)) but only in a minor amount (< 1  $\mu\text{M}$ ).

In addition to 7 $\alpha$ -dehydroxylation, *C. scindens* oxidized hydroxyl groups at the C3 and C7 positions on CA and CDCA molecules and additionally at the C12 position for CA (Figure 3). The oxidized secondary BAs produced include 3-oxoCA, 3-oxoCDCA, 3-oxoLCA, 7-oxoDCA, 7-oxoLCA,

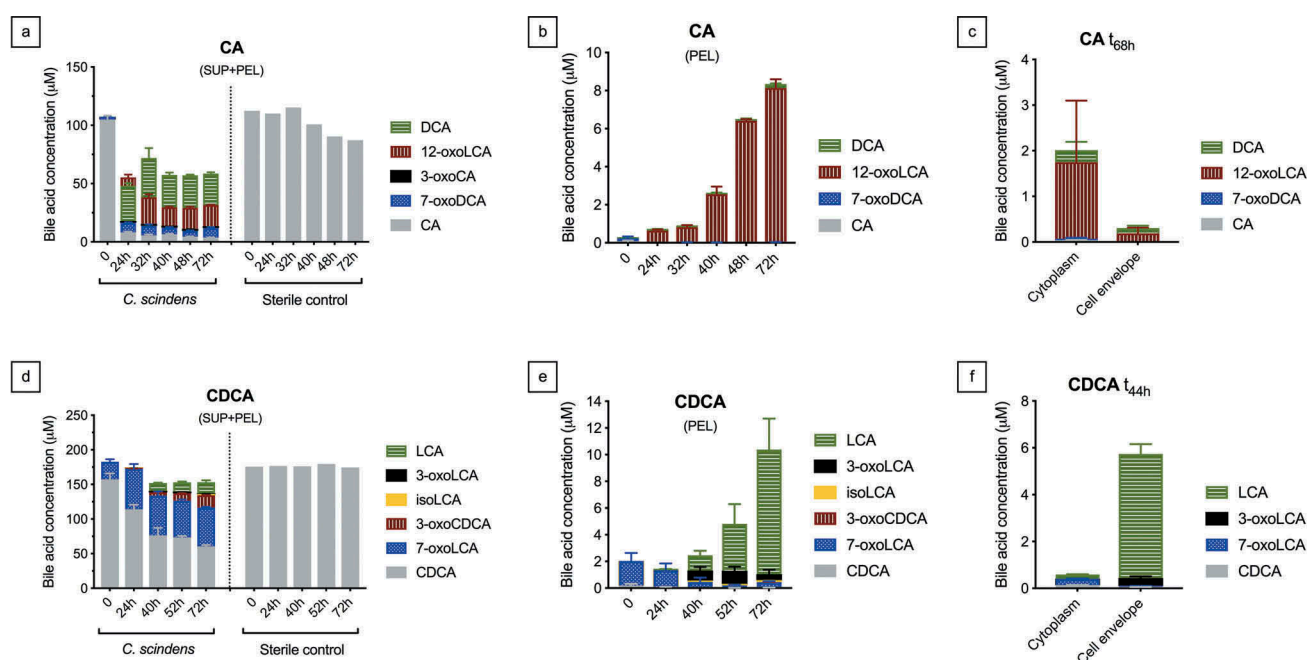


**Figure 3.** Bile acid transformations by *Clostridium scindens* *in vitro*. *C. scindens* was grown in BHIS-S containing either CA or CDCA in triplicates. Cultures were sampled and the pellet (PEL) separated from the supernatant (SUP) by centrifugation. Selected pellets were further fractionated into cytoplasmic and cell envelope fractions. Bile acids quantification is reported for the combined supernatant and pellet (SUP+ PEL) (a,d), for pellets (PEL) (b,e), and for the cytoplasmic and cell envelope fraction of the biomass (c,f). The analyses were carried out in triplicate, collected from triplicate cultures of *C. scindens*. Histograms indicate the mean and one standard deviation. Time zero represents the minimal amount of time needed to sample the culture, post bacterial amendment.

and 12-oxoLCA. Some of these secondary bile acid species, such as 12-oxoLCA (a product of CA transformation) are found in large quantities. 12-oxoLCA is formed rapidly and abundantly: at 24 h of incubation, 36% of CA was converted into 12-oxoLCA (Figure 3(a)). It represents the major cell-associated bile acid during CA transformation (Figure 3(b)) and is located in the cytoplasmic fraction (Figure 3(c)). Furthermore, between 24 h and 48 h of incubation, 12-oxoLCA decreased while DCA concentrations increased (Figure 3(a)).

In studies assessing bile acid transformations *in vitro*, the BA mass balance is not always achieved when measuring solution bile acids.<sup>31</sup> Hence, we quantified BAs in solution as well as associated with the cells. We found that about 10% and 5% of the CA- and CDCA-derived secondary bile acids are cell associated, respectively (Figures 3(b), 3(e)). After fractionation of the biomass, we observed that LCA was the only cell-associated BA that was primarily bound to the cell envelope (Figure 3(f)). *C. scindens* ATCC 35704 did not metabolize UDCA nor the two murine primary bile acids  $\alpha$ MCA and  $\beta$ MCA (Figure S1). In the experiments with CA, UDCA,  $\alpha$ MCA and  $\beta$ MCA (Figure 3(a) and S1), we noticed a decrease in the total bile acid concentration over time, both in the experimental and sterile control tubes. This decrease might be due to the adsorption of bile acids from the sample to walls of the epitube. In further experiments, all samples were extracted with alkaline acetonitrile, circumventing this experimental problem.

The formation of 12-oxoLCA and its accumulation intracellularly was unexpected as it is not an intermediate of the 7-dehydroxylation pathway<sup>32</sup> but rather described as an oxidized form of DCA.<sup>33–36</sup> In contrast, a known intermediate of the 7-dehydroxylation pathway, 3-oxoDCA, was not detected in the experiments (Figure 3). In order to better understand the formation of 12-oxoLCA, we performed additional *in vitro* experiments to investigate the transformation products of DCA, 3-oxoDCA, and 12-oxoLCA (Figure 4). We observed the oxidation of a small fraction of DCA (~ 11%) to 12-oxoLCA after 30 min followed by the reduction of 12-oxoLCA back to DCA within 36 h (Figure 4(a)). Regarding 3-oxoDCA, only a small fraction (~ 7%) was converted to DCA and this transformation was extremely slow

(Figure 4(b)). In contrast, 12-oxoLCA was rapidly and extensively converted to DCA (Figure 4(c)). After 6 h of incubation, the majority of 12-oxoLCA (~ 91%) was converted to DCA.

Bile acid 7-dehydroxylation is an intracellular process. In order to assess whether the limited transformation of DCA and 3-oxoDCA (Figures 4(a) and 4(b)) by *C. scindens* were due to inefficient transport of these BAs inside the cells, we performed an additional experiment using *C. scindens* cell-free extract (CFE) induced with CA before lysis and exposed to DCA or 3-oxoDCA (Figures 4(d) and 4(e)). CA is a known inducer of the expression of the *bai* operon encoding the 7-dehydroxylating enzymes.<sup>37</sup> The transformation of 12-oxoLCA by the CA-induced CFE was also assessed (Figure 4(f)). We observed that the CFE was more efficient at reducing 3-oxoDCA to DCA as compared to *C. scindens* whole cells (Figures 4(b) and 4(e)) despite corresponding to half the cell concentration ( $OD_{600} \sim 0.7$  instead of  $\sim 1.4$ ). The maximal DCA concentration with CFE was about 35  $\mu$ M after 10 h as compared to 5  $\mu$ M DCA after 60 h incubation with *C. scindens* whole cells. Interestingly, we detected a small fraction ( $\approx 1.35 \pm 0.06 \mu$ M after 10 h) of isoDCA, thus demonstrating the potential of *C. scindens* to epimerize the C3-hydroxyl group. Furthermore, another product of transformation of 3-oxoDCA was detected on the chromatogram with a  $m/z$  of 387.2523  $[M-H]^-$ , which could correspond to the elemental composition  $C_{24}H_{36}O_4$ , so a loss of two H atoms from 3-oxoDCA. Unfortunately, we did not have an appropriate standard to definitively identify and quantify this product based on its retention time, accurate mass and fragmentation pattern. This unknown product of 3-oxoDCA transformation could be 3,12-dioxoDCA, but further experiments will be needed to confirm this assignment.

The transformation of DCA by cell-free extract is similar to that with *C. scindens* whole cells. We observed the formation of a maximum of  $13.3 \pm 1.5 \mu$ M 12-oxoLCA with the CFE compared to  $12.8 \pm 1.2 \mu$ M with the whole cells (despite the factor of  $\sim 2$  less protein in the CFE system). However, the 12-oxoLCA formed by CFE remained in the medium and was not reduced back to DCA as observed with *C. scindens* whole cells (Figures 4(a) and 4(d)).

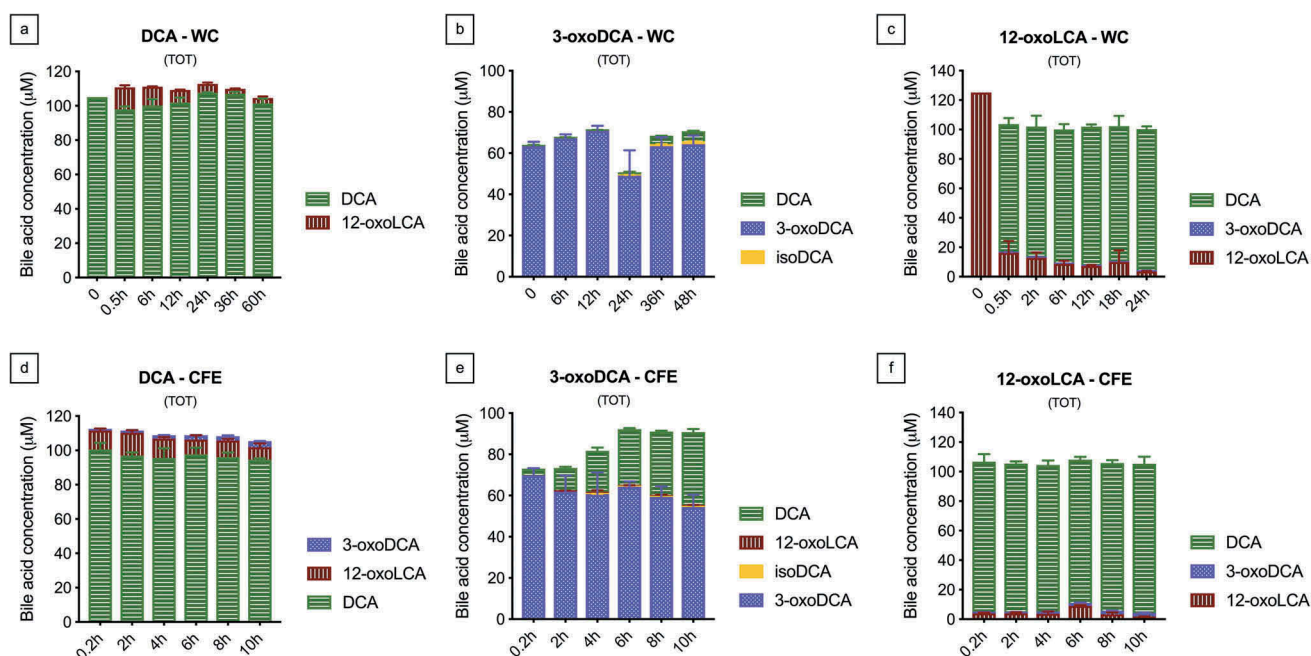


**Figure 4.** Secondary bile acid transformations by *Clostridium scindens* *in vitro* (whole cell and cell-free extract). Transformation products of the secondary bile acids DCA, 3-oxoDCA and 12-oxoLCA by whole *C. scindens* cells (WC) (a, b, and c). *C. scindens* was grown in BHIS-S containing one secondary bile acid (DCA, 3-oxoDCA, or 12-oxoLCA) in triplicate. Transformation products of the secondary bile acids DCA, 3-oxoDCA and 12-oxoLCA by CA-induced *C. scindens* cell-free extract (CFE) (d, e, and f). The synthesis of Bai enzymes was induced by the amendment of CA to a growing culture of *C. scindens*. The CA-induced cells were lysed and the cell-free extracts were amended with DCA, 3-oxoDCA or 12-oxoLCA. Each experiment was carried out in triplicates. Bile acids were extracted directly from the culture/CFE (supernatant and biomass), representing the total bile acids ('TOT'). Histograms indicate the mean and one standard deviation.

Furthermore, we detected the formation of a small amount of 3-oxoDCA ( $3.5 \pm 0.1 \mu\text{M}$  after 10 h of incubation) with CFE, which was not observed in the whole cell experiment (Figures 4(a) and 4(d)).

CFE reduced 12-oxoLCA rapidly and almost completely to DCA, similarly to our observation with *C. scindens* whole cells. In less than 30 minutes, almost all 12-oxoLCA ( $\sim 95\%$ ) was converted to DCA (Figure 4(f)).

### *Clostridium scindens* colonization and bile acid transformation in the murine intestinal tract

In order to investigate BA 7-dehydroxylation by *C. scindens* *in vivo* and its colonization dynamics, we used  $^{15}\text{N}$  and  $^{13}\text{C}$  labeled cells of *C. scindens*. We calibrated the decrease in  $\delta^{15}\text{N}$  and  $\delta^{13}\text{C}$  isotopic ratio as a function of division cycle by growing labeled *C. scindens* cells in unlabeled medium and monitoring the change in isotopic ratio (Figure S2). As expected, the isotopic ratios

( $^{13}\text{C}/^{12}\text{C}$  and  $^{15}\text{N}/^{14}\text{N}$ ) of individual *C. scindens* cells are halved at each cell division as individual cells undergo symmetric division taking up normal composition N and C from the medium. Once the stationary phase is reached and the cells stop dividing, the isotopic ratios remain quasi constant (Figure S2). The nitrogen isotopic ratio is 3 times greater than the carbon ratio and was selected for further analyses because it affords more resolution of bacterial division.

The  $^{15}\text{N}$  isotopically labeled *C. scindens* cells were used to complement the intestinal microbial community of mice from a gnotobiotic mouse line (sDMDMm2) devoid of 7-dehydroxylating strains.<sup>38,39</sup> Six hours after inoculation by gavage of  $10^9$  cells, *C. scindens* was already detectable in the distal intestinal tract (Figure 5). *C. scindens* concentrations were low in the jejunum and ileum compared to the large intestine. In the small intestine, *C. scindens* numbers were below detection by cultivation at 6 h. At 24 h, there was on average of  $6.5 \pm 5.7 \times 10^2$  CFU of *C. scindens* per g of intestinal content in the ileum



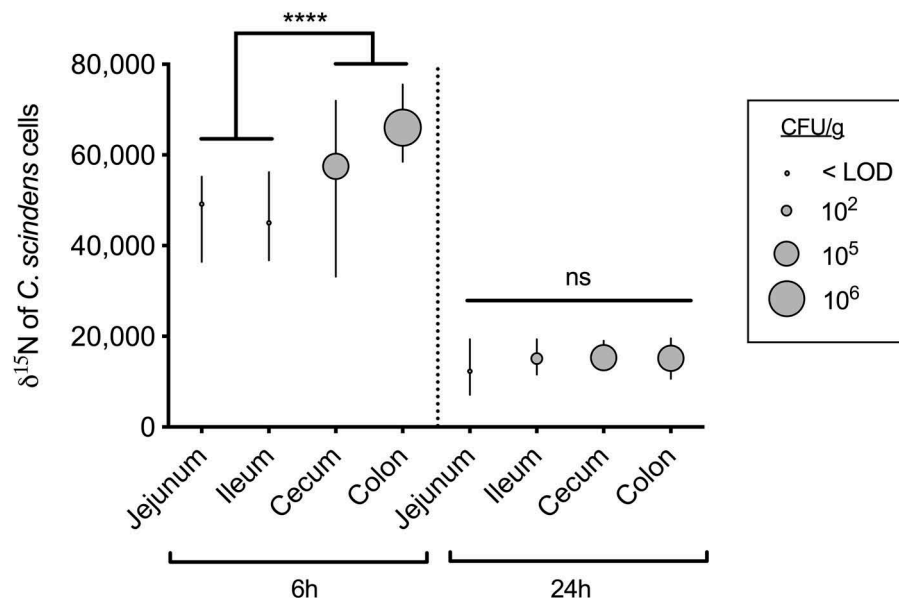


**Figure 5.** *Clostridium scindens* colonizes the large intestine of the murine gut. *C. scindens* was grown *in vitro* in a medium with  $^{15}\text{N}$ -labeled nutrients and gavaged into sDMDMm2 mice. A control culture was obtained in a medium lacking labeled compounds (unlabeled). The nitrogen isotopic ratio of *C. scindens* along the intestinal tract was quantified from NanoSIMS images. Samples from two mice (one per time point) were analyzed. *C. scindens* concentration (CFU/g of intestinal content) were determined by plating on selective medium. The y-axis indicates  $^{15}\text{N}$  isotopic ratio of *C. scindens* cells. The bubble centers indicate medians and the vertical bars the interquartile range. The size of the bubbles indicates *C. scindens* concentrations. Statistical analysis used Mann-Whitney-U tests to compare the *C. scindens* isotopic ratios in the small and large intestine. Ns, not statistically significant ( $p \geq 0.05$ ), \*\*\*\* $p < 0.0001$ . < LOD implies that the value is below the limit of detection.

only. In contrast, the cell counts were  $6.1 \pm 8.6 \times 10^5$  and  $3.2 \pm 4.9 \times 10^5$  CFU of *C. scindens* per g of intestinal content at 6 h and 24 h, respectively for the cecum. In the colon, the cell counts were  $4.6 \pm 6.4 \times 10^6$  at 6 h and at 24 h they were comparable to those in the cecum ( $7.2 \pm 11.5 \times 10^5$ )

The nitrogen isotopic ratio of the *C. scindens* gavage culture equaled 420,600 (Figure S3). Thus, within the gut microbial community of sDMDMm2 mice, *C. scindens* cells, were readily detected using the NanoSIMS-generated  $^{12}\text{C}^{15}\text{N}^-$  and  $^{12}\text{C}^{13}\text{C}^-$  images (Figure S4).

The nitrogen isotopic ratio of *C. scindens* cells decreased rapidly overtime in the intestinal tract (Figure 5). After 6 h, the ratios were significantly lower in the small intestine compared to the large intestine, suggesting that cells in the large intestine underwent fewer bacterial divisions than those in the small intestine. Twenty-four hours after gavage, the isotopic ratios were lower than at 6 h, suggesting that cells continued to divide in all intestinal compartments. There is no statistically significant difference among the compartments at

24 h indicating that *C. scindens* cells underwent a similar number of bacterial divisions. However, only considering the nitrogen isotope ratios provides an incomplete view of the process because it does not take into account the fact that the number of cells present in the ileum is three orders of magnitude smaller than that in the cecum or colon. Hence, while the small number of cells present in the ileum (and to a lesser extent, the jejunum) divides at the same rate at those in the cecum and colon, they represent a small population. Thus, the great majority of *C. scindens* cells has colonized the large intestine and are dividing and growing in that compartment.

We analyzed the bile acid profile along the intestinal tract of sDMDMm2 mice and sDMDMm2 mice colonized with *C. scindens* to explore the impact of *C. scindens* on the bile acid metabolome. Figure 6 shows that the luminal bile acid concentrations vary greatly along the murine intestinal tract. The bile acid pool in the large intestine represents about 5% of that in the small intestine. In the small intestine, the bile acid

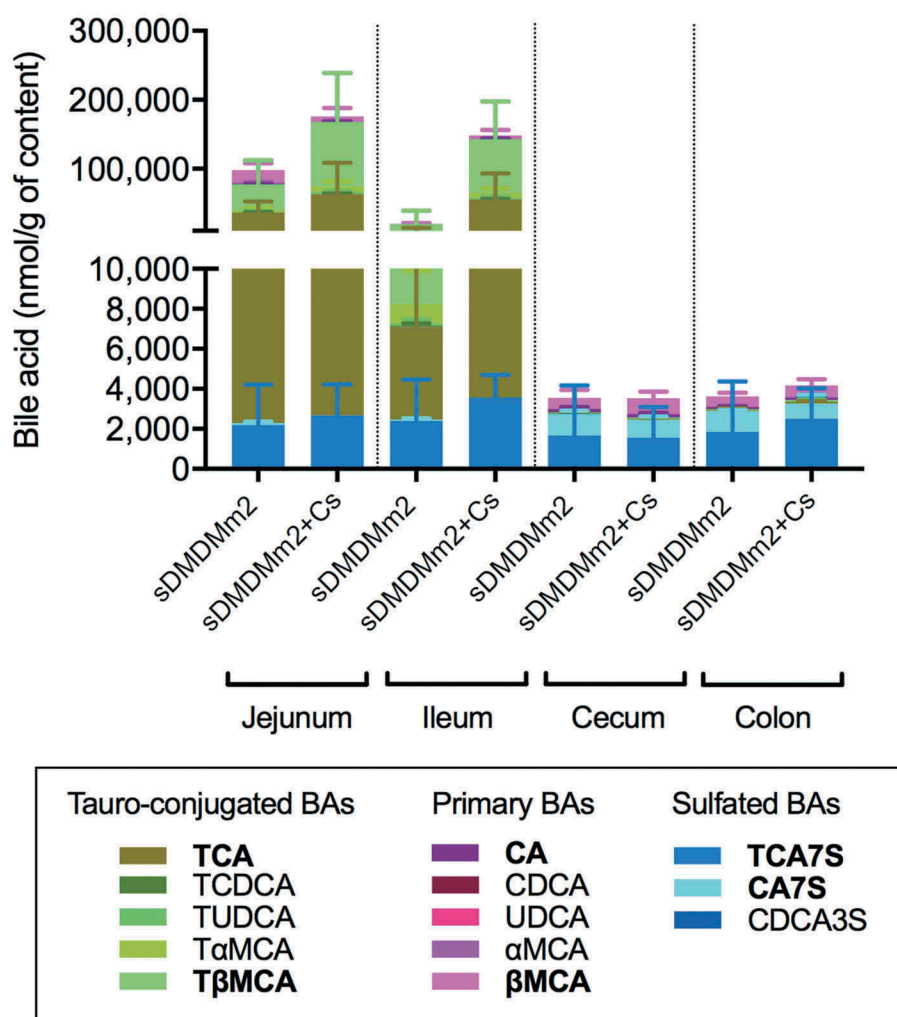


**Figure 6.** Luminal bile acid composition along the intestinal tract of sDMDMm2 mice colonized with *C. scindens* (sDMDMm2+ Cs) compared to sDMDMm2 control mice. Bile acids were analyzed with UHPLC-HRMS in four intestinal compartments collected from sDMDMm2 mice colonized with *C. scindens* for 24h (n = 3, sDMDMm2+ Cs) and a control group (n = 3, sDMDMm2) that received a PBS vehicle. The legend indicates the bile acids detected. The ones abundant enough to be visible on the graph are in bold in the legend. The secondary bile acids are depicted in Figure 7 and 8.

composition is largely accounted for by conjugated species: TCA, TβMCA, as well as tauro-conjugated cholic acid sulfated at the C7 position (TCA7S). In the large intestine, we observe the efficient deconjugation of bile acids, with the major remaining species consisting mainly of sulfated cholic acids (CA7S and TCA7S) and βMCA.

The presence of these unconjugated bile acids in the large intestine allows further transformations, including the epimerization of the hydroxyl group at the C6 position (producing ωMCA), and the oxidation of the hydroxyl groups at the C3 and C7 positions (producing 3-oxoCA, 3-oxoCDCA, 7-oxoDCA, and

7-oxoLCA) (Figure 7).<sup>18</sup> These transformations occur in the presence and absence of *C. scindens*, suggesting that members of the sDMDMm2 microbial community are responsible. Furthermore, the concentrations of these unconjugated secondary BAs are not significantly different in the large intestine of *C. scindens*-colonized sDMDMm2 mice relative to control mice (sDMDMm2) (Figure 7).

There is one bile acid species that is only present in the mouse with the *C. scindens*-amended microbiota: DCA (Figure 8). This is the 7-dehydroxylated form of CA. This result is consistent with the 7-dehydroxylating activity of *C. scindens* and confirms the

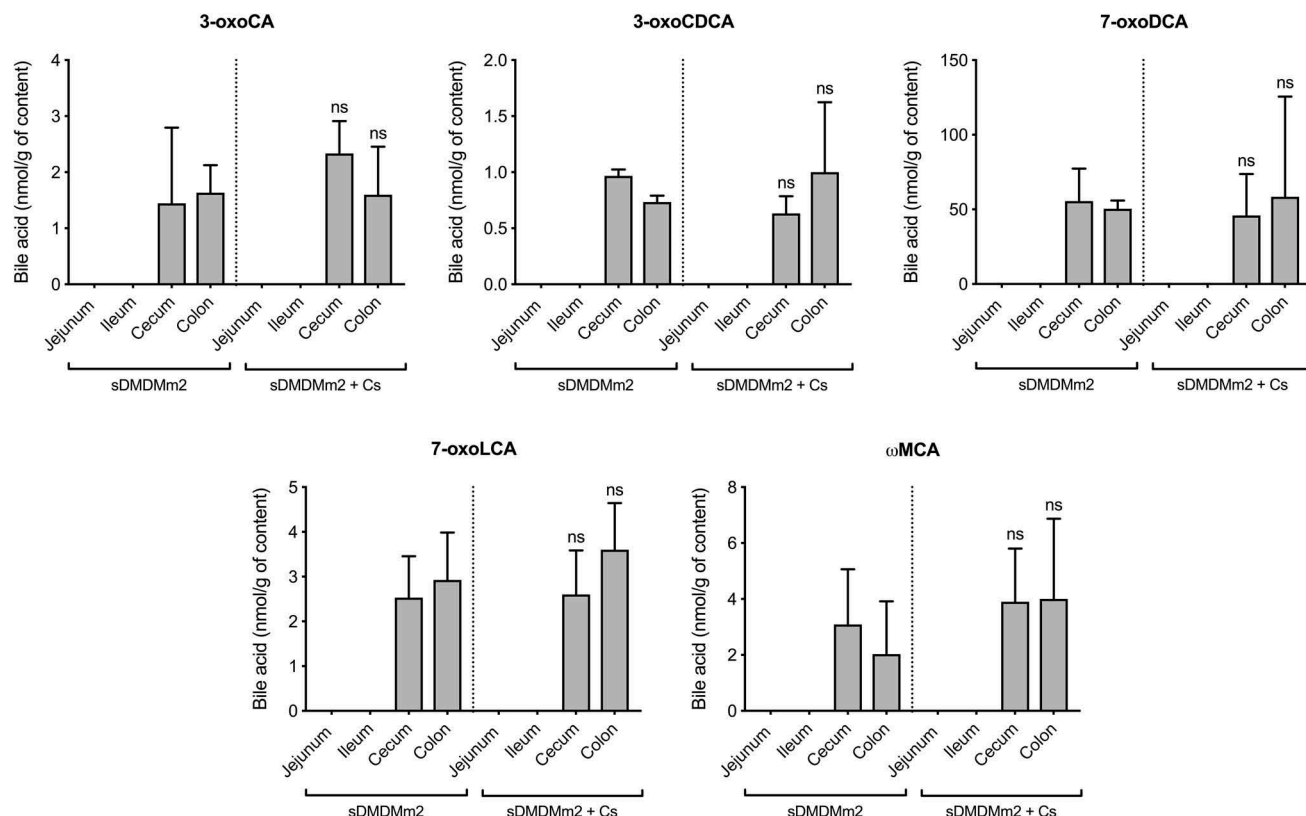


**Figure 7.** Secondary bile acid composition along the intestinal tract of sDMDMm2 mice colonized with *C. scindens* compared to control sDMDMm2 mice. Bile acids were analyzed with UHPLC-HRMS in four intestinal compartments collected from sDMDMm2 mice colonized with *C. scindens* for 24h ( $n = 3$ , sDMDMm2+ Cs) and a control group ( $n = 3$ , sDMDMm2) that received PBS vehicle. Statistic analysis used the Mann-Whitney-U tests to compare the secondary bile acid concentrations in mice colonized with *C. scindens* to a control sDMDMm2 mouse. Histograms indicate the mean with the standard deviation. ns, not statistically significant ( $p \geq 0.05$ ). A value of zero indicates that the concentration is below the limit of detection.

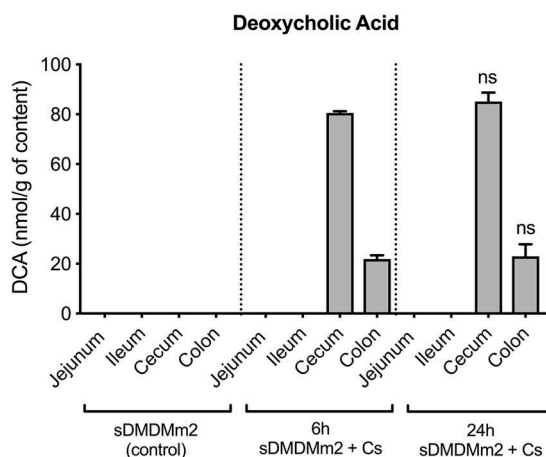


**Figure 8.** Deoxycholic acid (DCA) formation *in vivo* as a function of time. DCA was quantified with UHPLC-HRMS in four intestinal compartments (jejunum, ileum, cecum and colon) collected from sDMDMm2 mice colonized with *C. scindens* for 6h ( $n = 3$ , sDMDMm2+Cs) and 24h ( $n = 3$ , sDMDMm2+Cs) and a control group ( $n = 3$ , sDMDMm2) that received PBS vehicle. Histograms indicate the mean with the standard deviation. Mann-Whitney-U tests were performed to compare DCA levels between  $T_{6h}$  and  $T_{24h}$ . ns, not statistically significant ( $p \geq 0.05$ ). A value of zero indicates that the concentration is below the limit of detection.

colonization data. The amount of DCA is stable over time in the cecum and colon (Figure 8).

## Discussion

Bile acids exhibit detergent properties. In the small intestine, they form micelles and promote dietary lipid solubilization and absorption. When present at high concentrations, bile acids can be cytotoxic to the bacteria and the host. The intestinal bile acid pool (size and composition) is known to structure the microbial community along the intestinal tract and therefore plays an important role in maintaining the intestinal barrier function.<sup>40–42</sup>

Bile acid 7-dehydroxylating bacteria represent an important functional group amongst bile-transforming gut bacteria. They produce 7-dehydroxylated secondary bile acids, which represent a major fraction of the secondary bile acids pool (~ 64% in the cecum of the *C. scindens* colonized sDMDMm2 mice). 7-dehydroxylated bile acids, such as DCA and LCA, are potent activators of the bile acid receptor TGR5, and consequently are involved in the regulation of glucose homeostasis, energy expenditure and inflammation.<sup>3,4,43</sup> Bile acid 7-dehydroxylating bacteria thus may represent a critical link between bile acids and host health.<sup>5</sup> As such, they could be a target for the prevention and treatment of various metabolic diseases<sup>9</sup>, as well as *Clostridium difficile* infections (CDI)<sup>7</sup> and some gastrointestinal cancers, which are associated with increased levels of 7-dehydroxylated bile acids.<sup>44</sup> Using 7-dehydroxylating bacteria for therapeutic or preventative applications requires a better understanding of their microbiology *in vivo* as well as their interactions with the host. In the present study, we explored the bile acid metabolism of *C. scindens*, a known 7-dehydroxylating bacterium, both *in vitro* and *in vivo* and investigated its colonization dynamics in the murine intestinal tract.

The growth of *C. scindens* ATCC 35704 was not impacted by the primary or secondary bile acids tested *in vitro* (Figures 2(a), 2(b)). A notable exception is CDCA, which revealed a toxic effect (Figure 2(a)), as is expected because it is a hydrophobic bile acid.

*C. scindens* metabolized CA and CDCA *in vitro* and the products of their transformation were primarily recovered from solution. A notable exception is LCA, which was associated with the cell envelope, underscoring its hydrophobicity, and another is 12-oxoLCA, which was recovered from the cytoplasm, suggesting it is not effectively effluxed by the cell (Figure 3). CA was more efficiently dehydroxylated than CDCA (Figure 3(a)), as was previously reported for *C. hiranonis*<sup>31</sup> and *C. scindens* VPI 12708.<sup>30</sup>

In contrast, the murine primary bile acids  $\alpha$ MCA and  $\beta$ MCA remained unchanged (Figure S1), confirming previous reports that human intestinal bacteria are unable to metabolize muricholic acids.<sup>17,45</sup> A possible explanation for this is host specificity as *C. scindens* may have evolved in the human gut in the absence of murine primary bile acids. However, *C. scindens* may not be an exclusively human commensal as a new strain (strain G10) was recently isolated from rat feces.<sup>25</sup> The 7 $\beta$ -dehydroxylation of UDCA was also tested *in vitro*. This transformation was previously reported for several 7-dehydroxylating organisms including several *C. scindens* strains (VPI 12708, 36S, M-18, Y-98, Y-1112, Y-1113) and *Eubacterium* strain C-25.<sup>31,46</sup> The gene *bail* is predicted to encode a 7 $\beta$ -dehydratase<sup>47</sup> but this remains to be confirmed as this process could also occur *via* a 7 $\beta$ -epimerization to CDCA followed by 7 $\alpha$ -dehydroxylation. Here, we did not observe any conversion of UDCA by *C. scindens* ATCC 35704 *in vitro* (Figure S1), consistent with previous reports.<sup>48</sup>

*In vitro*, *C. scindens* also oxidized the C3 and C7 hydroxyl groups in CA and CDCA, yielding 3-oxoCA and 7-oxoDCA (for CA) and 3-oxoCDCA and 7-oxoLCA (for CDCA) (Figure 3). In addition, 7-dehydroxylation was combined with oxidation, to produce 12-oxoLCA for CA and 3-oxoLCA for CDCA, and with epimerization to produce isoLCA. Oxidation at C3, C7 and C12, as well as 7 $\alpha$ - and 7 $\beta$ -dehydroxylation of the C7 hydroxyl group by various *C. scindens* strains have all been previously reported.<sup>23,30–32,46,48,49</sup> Thus, these findings are in line with the expected composition of the products of CA and CDCA incubations with *C. scindens*. In contrast, it is the first time that epimerization of the C3-hydroxyl of LCA to isoLCA (3 $\beta$ ) is reported for *C. scindens* perhaps due to its presence at a low concentration ( $\leq 2\mu\text{M}$ ). While *Clostridium scindens*

carries several 3 $\alpha$ -hydroxysteroid dehydrogenase (3 $\alpha$ -HSDH) on the *bai* operon (BaiA enzymes)<sup>50</sup>, 3 $\beta$ -HSDH has never been characterized for this organism.

The BA 7-dehydroxylation pathway invokes the oxidation of the C3 hydroxyl, followed by the oxidation of the C4-C5 bond, the dehydration at the C7 hydroxyl, the reduction of the C4-C5 and C6-C7 bonds, and finally the reduction of the C3 ketone group.<sup>32</sup> Thus, a 3-oxoDCA intermediate is involved in the pathway.<sup>51</sup> However, we did not detect it in our experiment (Figure 3) nor is it reported as a product of CA transformation by *C. scindens* in a recent study, while it is detected during CA 7-dehydroxylation by *C. hiranonis*.<sup>52</sup> In the same study, no transformation of 3-oxoDCA into DCA (as would be expected based on the pathway) is detected in any of the 7-dehydroxylating strains considered.<sup>52</sup> Similarly, our results show that *C. scindens* converted a minor part of 3-oxoDCA (7%) to DCA (Figure 4 (b)). *C. scindens* has several copies of the *baiA* gene encoding 3 $\alpha$ -HSDH enzymes<sup>50</sup>, thus it is unclear whether the lack of 3-oxoDCA reduction is due to limited expression of the 3 $\alpha$ -HSDHs or to the lack of transport of 3-oxoDCA into the cell. To circumvent these possible confounding effects, we used CA-induced *C. scindens* CFE to interrogate 3-oxoDCA transformation. Reduction of 3-oxoDCA ensued (39% at 10 h), resulting in increased production of DCA compared to that with whole cells (Figure 4 (e)). These results confirm that 3-oxoDCA is a likely intermediate in the formation of DCA and that its intracellular intake is limited.

An unanticipated finding was the transformation of CA into 12-oxoLCA (Figure 3(a)). This secondary bile acid has not been reported in previous CA 7-dehydroxylation experiments with *C. scindens*.<sup>52</sup> We observed a transient accumulation of this bile acid in the biomass during CA transformation *in vitro* (Figure 3(b)). Interestingly, this bile acid species accumulated in the cytoplasm of the cells (Figure 3(c)). In the literature, this secondary bile acid is described as a product of the oxidation of DCA.<sup>33–36,53</sup>

We investigated the transformation of 12-oxoLCA by *C. scindens* to determine whether 12-oxoLCA may be reduced to DCA. The transformation of 12-oxoLCA to DCA by both whole cells and CFE was very rapid (86% in 2 h and 95% in less than 30 minutes, respectively), suggesting high 12 $\alpha$ -

HSDH activity (Figures 4(c) and 4(f)). Similarly, Doden *et al.* (2018) report complete conversion of 12-oxoLCA to DCA by the three major 7-dehydroxylating species *C. scindens*, *C. hylemonae* and *C. hiranonis*.<sup>52</sup>

In contrast, DCA transformation to 12-oxoLCA by *C. scindens* whole cells was slow (11.5% in 30 minutes) and the 12-oxoLCA produced was converted back to DCA (< 3% remaining at 36 h) (Figure 4(a)). This is consistent with previous work by Winter *et al.* (1984) and Doden *et al.* (2018)<sup>52</sup> who reported no conversion of DCA by *C. scindens* strain ATCC 35704.<sup>48</sup> To address the possible confounding issues of expression of the 12 $\alpha$ -HSDH in the presence of DCA and of the potentially limited uptake of DCA by cells, CA-induced *C. scindens* CFE was exposed to DCA and a minor transformation of DCA to 12-oxoLCA (11.8% in 12 min) was observed, similar to that with *C. scindens* whole cells after 30 minutes. However, the 12-oxoLCA formed by CFE was not converted back to DCA over time (Figure 4 (d)). These results suggest that 12-oxoLCA could be a transient species during CA 7-dehydroxylation to DCA, which is incompatible with the 7-dehydroxylation pathway.<sup>32</sup> Further investigations are needed to elucidate the occurrence of this secondary bile acid species, its connection with the 7-dehydroxylation pathway, and its role on host physiology.

Overall, the *in vitro* transformation of CA by *C. scindens* involves BA 7-dehydroxylation to both reduced (DCA and isoDCA) and oxidized (12-oxoLCA, 3-oxoDCA) secondary BAs as well as oxidation of primary BAs (7-oxoDCA, 3-oxoCA) (Figure 9). Similarly for CDCA, reduced (LCA and isoLCA) and oxidized (3-oxoLCA) 7-dehydroxylated species are formed along with oxidized primary BAs (7-oxoLCA, 3-oxoCDCA) (Figure 10). The 3-oxo, 7-dehydroxylated species (3-oxoDCA and 3-oxoLCA) are intermediates in the known 7-dehydroxylation pathway, whereas the 12-oxo, 7-dehydroxylated species (12-oxoLCA) is likely to be a transient species formed during CA 7-dehydroxylation. The 7-oxo species are not substrates for 7-dehydroxylation<sup>32</sup> and require reduction back to the primary BA for further transformation by *C. scindens* (Figures 9 and 10).



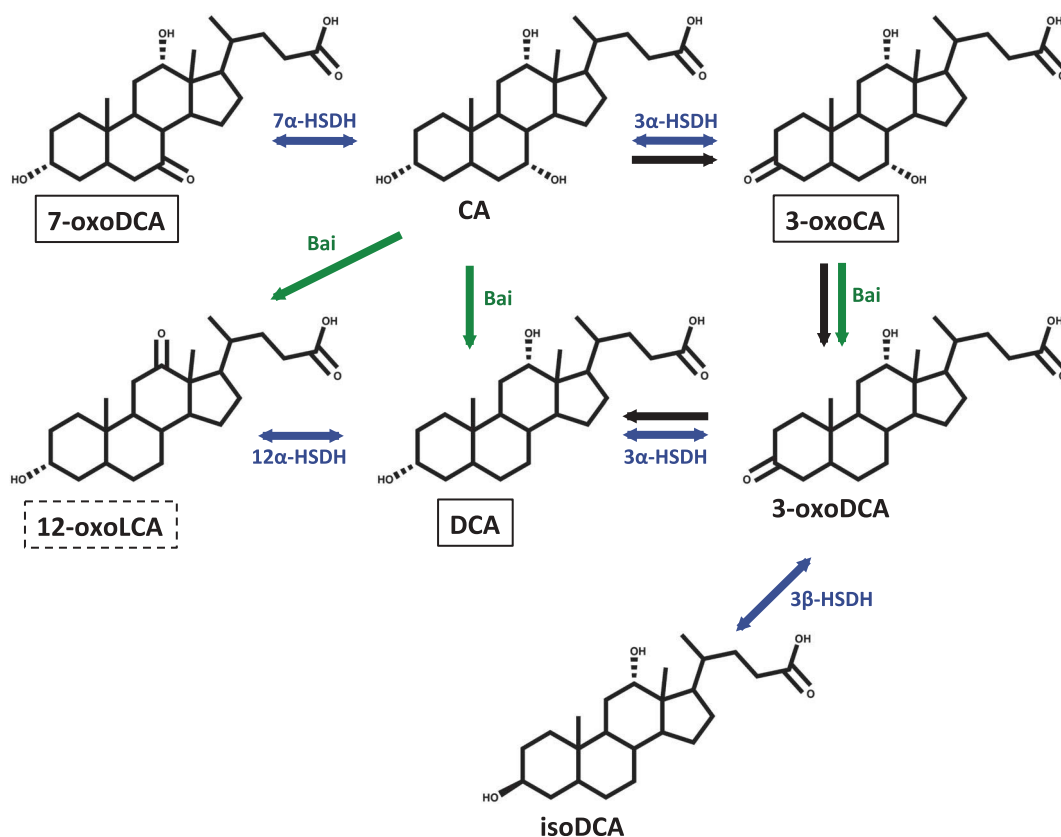


**Figure 9.** Cholic acid (CA) transformations carried out by *Clostridium scindens* *in vitro* and *in vivo*. The secondary bile acids produced by *C. scindens* *in vitro* are indicated and those that were also detected *in vivo* are in boxes. The dashed boxes indicate those reported *in vivo* in the study from Studer *et al.* (2016), using the same gnotobiotic mouse model (sDMMm2 + *C. scindens*).<sup>39</sup> The black arrows indicate the 7-dehydroxylation pathway and its BA intermediates. The green arrows depict bile acid 7-dehydroxylation and the blue bidirectional arrows show the oxidation/reduction transformations. Enzymes catalyzing these transformations are indicated next the arrows. Bai stands for the enzymes of the *bai* operon involved in the 7-dehydroxylation.

In order to evaluate the relevance of *C. scindens* *in vitro* bile acid transformations *in vivo*, we amended a gnotobiotic mouse model with <sup>15</sup>N- and <sup>13</sup>C-labeled *C. scindens* cells and analyzed the bile acid metabolome along the intestinal tract. In parallel, we probed the *in vivo* colonization behavior of *C. scindens* by following the cell isotopic ratios in the mouse intestine using NanoSIMS. The selected gnotobiotic mouse model (sDMMm2) is associated with a stable, low-complexity microbiota consisting of 12 species belonging to the main phyla of the murine gut microbiota and devoid of 7-dehydroxylation capability.<sup>38</sup> Thus, by amending the model microbiota with *C. scindens*, we aimed to restore bile acid 7-dehydroxylation. This complemented mouse model (sDMMm2 + *C. scindens*) was previously reported by our group.<sup>39</sup> However, it is the first time the bile acid profile

along the intestinal tract (jejunum, ileum, cecum and colon) of this mouse model is documented.

The bile acid composition along the gut in mice colonized with *C. scindens* and in the control mouse confirms previous observations that approximately 95% of the bile acid pool is reabsorbed into the distal ileum as part of the enterohepatic recirculation and that only 5% enters the large intestine (Figure 6).<sup>54</sup> Additionally, we observe a rapid conversion of CA to DCA in the mice colonized with *C. scindens* (Figure 8) while, as expected, DCA is absent in mice that are not colonized with *C. scindens*. Hence, the amendment of *C. scindens* to the sDMMm2 mice microbial community partly restores the expected bile acid composition by allowing 7 $\alpha$ -dehydroxylation, as previously shown.<sup>39</sup> As expected, all the secondary bile acids detected *in vivo* (Figures 7 and 8) were not detected in germ-free mice<sup>39</sup>, highlighting the role of microorganisms in the synthesis of secondary bile acids.

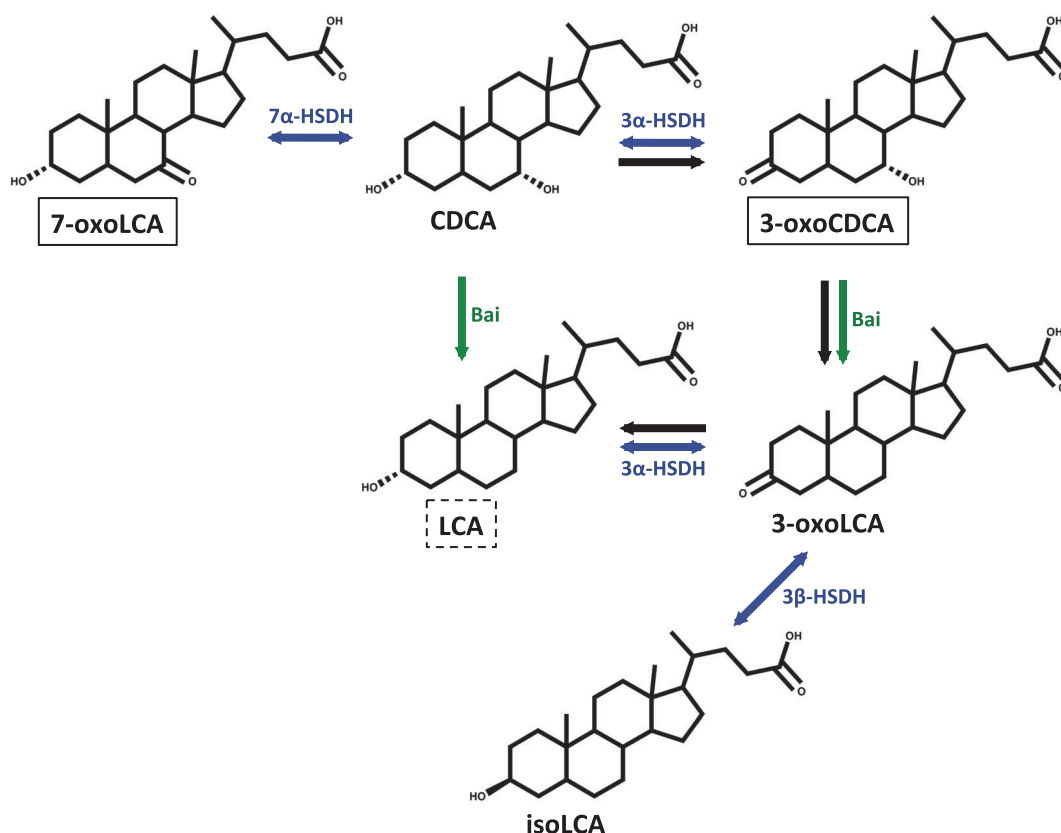


**Figure 10.** Chenodeoxycholic acid (CDCA) transformations carried out by *Clostridium scindens* *in vitro* and *in vivo*. The secondary bile acids produced by *C. scindens* *in vitro* are indicated and those that were also detected *in vivo* are in boxes. The dashed boxes indicate those reported *in vivo* in the study from Studer *et al.* (2016), using the same gnotobiotic mouse model (sDMMdm2 + *C. scindens*).<sup>39</sup> The black arrows indicate the 7-dehydroxylation pathway and its BA intermediates. The green arrows point out the bile acid 7-dehydroxylation and the blue bidirectional arrows show the oxidation/reduction transformations. Enzymes catalyzing these transformations are indicated next the arrows. Bai stands for the enzymes of the *bai* operon involved in the 7-dehydroxylation.

Interestingly, in contrast to our observations *in vitro* (Figure 3(d)) and the study from Studer *et al.* (2016)<sup>39</sup>, there was no evidence of LCA, suggesting that *C. scindens* did not 7-dehydroxylate CDCA *in vivo* (Figure 6). This discrepancy could be attributed to the short colonization time with *C. scindens* (24 h). Studer *et al.* (2016) colonized the mice with *C. scindens* for 7 days. Similarly, 12-oxoLCA was reported in the cecum of sDMMdm2 mice colonized with *C. scindens* for 7 days but not detected in this study. A longer colonization time (> 24 h) with *C. scindens* might be required for the production of certain secondary bile acids (e.g., LCA and 12-oxoLCA). Other secondary bile acids formed from CDCA (e.g., 3-oxoCDCA and 7-oxoLCA) were detected in the cecum and colon of the mice and taken together, these secondary bile acids are found at the same concentration as CDCA, suggesting that half of the CDCA bile acid pool was oxidized (at C3

and C7). Oxidation of CDCA was also found to exceed 7-dehydroxylation *in vitro* (Figure 3(d)). A possible explanation for this might be that the enzymes oxidizing bile acids (HSDH) are more abundantly expressed than the 7-dehydroxylating enzymes (encoded by *bai* genes) within the gut microbial community.<sup>55</sup> Further, consistent with the *in vitro* data (Figure S1), *C. scindens* did not use muricholic acids as substrates for 7-dehydroxylation *in vivo* (Figure 6). In contrast to the *in vitro* data, iso-secondary bile acids were not detected in the mice. The concentrations of isoLCA and isoDCA detected *in vitro* were low (< 2 $\mu$ M), thus the epimerization of C3-hydroxyl is a minor transformation of *C. scindens*. In humans, other bacteria, such as *Eggerthella lenta* and *Ruminococcus gnavus*, likely contribute to the formation of iso (3 $\beta$ -hydroxyl) bile acids which are reported to be the second most abundant class of bile acids in the gut.<sup>56</sup>

*In vivo*, we observed that the concentrations of secondary bile acids (3-oxoCA, 3-oxoCDCA, 7-oxoDCA, 7-oxoLCA and  $\omega$ MCA) were comparable between *C. scindens*-colonized sDMDMm2 mice and the control sDMDMm2 mice (Figure 7). Thus, in the large intestine, *C. scindens* restores bile acid 7-dehydroxylation without affecting the rest of the bile acid pool. In line with this observation, our group recently reported that *C. scindens* association had only a minor impact on the composition of the sDMDMm2 microbiota.<sup>39</sup>

To explore the colonization dynamics of this 7-dehydroxylating bacterium in the murine intestinal tract, mice were inoculated with isotopically labeled *C. scindens* cells (with <sup>15</sup>N and <sup>13</sup>C) and their isotopic signatures along the gut were measured with NanoSIMS (Figure S4). As bacteria grow, the N or C isotopic ratio of *C. scindens* cells decreases because C and N with normal isotopic composition is taken up, diluting the isotopic signature (Figure S2). Thus, based on the cells isotopic ratios, we can infer the average number of cell divisions and hence, determine whether the cells present at that location have grown relative to previous time point. Given that the cells were delivered in a single gavage, we surmise that to remain in the intestinal tract, their growth rate must exceed the rate of cell death and loss through feces. Hence, only cells that colonize the intestine should be able to divide once the bolus has passed through the intestinal tract (< 6 h). We found that cell growth was detectable in all compartments, suggesting colonization throughout the intestinal tract but cell numbers were vastly different in the small and large intestines. In the small intestine, *C. scindens* numbers were below detection limit by cultivation at 6 h. At 24 h, there was about 10<sup>2</sup>-10<sup>3</sup> CFU of *C. scindens* per g of intestinal content in the ileum only. In contrast, the cell counts ranged between 10<sup>4</sup>-10<sup>7</sup> CFU of *C. scindens* per g of intestinal content at 6 h and 24 h, for the cecum and colon (Figure 5).

Interestingly, the isotopic ratios of *C. scindens* cells were lower in the small intestine than in the large intestine at 6 h, suggesting that cells underwent more bacterial divisions in the small than in the large intestine (Figure 5). Thus, there are fewer cells colonizing the small intestine than the cecum or colon but those that have colonized appear to divide more rapidly at the initial time point. Considering the large inoculum administrated into the mice and intestinal motility, we

interpret these results as representing the arrival of cells from the inoculum (with high isotopic values, Figure S3) to the large intestine. It is common that large inocula undergo a 'lag phase' *in vivo* following administration before colonization starts. The bolus, dominated by slowly proliferating bacteria, transits through the gastrointestinal tract and seeds bacteria that start to genuinely colonize and proliferate. The bacteria in the small intestine at 6 h arrived a few hours earlier than those in the large intestine, thus have undergone more bacterial division and have lower isotopic ratios. We hypothesize that colonization of the small intestine is generally unfavorable but that there are micro-environments in which the 7-dehydroxylating cells live and divide, particularly in the ileum. After 24 h, the isotopic ratio is similar across the entire intestinal tract reflecting the steady-state colonization of the gut but the overwhelming majority of the 7-dehydroxylating biomass remains in the large intestine. This study also demonstrates the potential of NanoSIMS technology to track a bacterium of interest in a host.<sup>57-59</sup>

We demonstrated that *C. scindens* could divide in the small intestine and persist in small numbers (Figure 5). However, the large intestine is its primary ecological niche, and it is where *C. scindens* efficiently performs CA 7-dehydroxylation to DCA *in vivo* (Figure 8). DCA was not detected in the small intestine despite the presence of actively growing *C. scindens* 6 h after gavage, based on NanoSIMS analysis (Figure 5). Several factors may have impacted bile acid 7-dehydroxylation in the small intestine. The most parsimonious explanation is that bile acids in the small intestine are conjugated (Figure 6), which precludes 7-dehydroxylation.<sup>18</sup> The gnotobiotic sDMDMm2 mice have an efficient deconjugating community in the large intestine, as most bile acids are deconjugated (Figure 6). Thus, *C. scindens* cells have access to unconjugated primary BAs that can be dehydroxylated, which is not the case in the small intestine.

Interestingly, the majority of the primary BAs in the cecum and colon are sulfated (76% in *C. scindens*-colonized sDMDMm2 mice) while only a small fraction (3% in *C. scindens*-colonized sDMDMm2 mice) of the small intestine BAs exhibits this modification (Figure 6). Bile acid sulfation at the C3 and C7 positions has been suggested to represent a detoxification

strategy<sup>60</sup> as it effectively increases their solubility, decreases the intestinal reabsorption and consequently promotes their elimination in feces and urine.<sup>60</sup> However, it has been shown that this modification precludes 7-dehydroxylation if the sulfate group is associated with the hydroxyl group at the C7 position.<sup>61</sup>

Thus, the colonization dynamics appear to confirm the work by Midvedt and Norman (1968) where they considered the spatial distribution of the bile acid transformations along the rat intestinal tract. Bile acid 7-dehydroxylating bacteria were found in the cecum but not in the ileum of three conventional rats.<sup>14</sup> Fifty years later, we confirm that the bile acid 7-dehydroxylating bacterium *C. scindens* colonizes primarily the large intestine of gnotobiotic mice but we also report limited colonization of the ileum (Figure 5). However, it is clear that the activity of 7-dehydroxylating bacteria is only detectable in the large intestine, presumably due to the exclusive availability of deconjugated bile acids in that intestinal compartment.

## Conclusion

This study provides insight into the microbiology of 7-dehydroxylating organisms. First, the detailed analysis of bile acid transformations catalyzed by *C. scindens* allowed the uncovering of a novel intermediate, 12-oxoLCA. It is unclear how this intermediate fits into the well-established 7-dehydroxylation pathway. Further investigations are required to further unravel the role of this compound in 7-dehydroxylation. Furthermore, we have shown that DCA and LCA are products of primary bile acid metabolism by *C. scindens* (as expected) but also that other 7-dehydroxylated species form (e.g., 3-oxoLCA, 12-oxoLCA, isoDCA and isoLCA) and should be accounted for in the pool of 7-dehydroxylated product. The partitioning of bile acids into the cell envelope occurs for the more hydrophobic species and should also be considered for bile acid mass balance purposes. Finally, investigation of the dynamics of colonization of *C. scindens* in the gut using NanoSIMS has confirmed the primarily cecal and colonic localization of 7-dehydroxylating bacteria but has also evidenced the colonization of

the ileum by a small number of *C. scindens* cells. There is no evidence of bile acid 7-dehydroxylation in that compartment but growth can clearly take place fuelled by fermentative processes.

## Material and methods

### Oligo-MM<sup>12</sup> microbiota and gnotobiotic sDMDMm2 mice

The sDMDMm2 gnotobiotic mouse model was used in this study. sDMDMm2 mice are colonized with a mouse-intestine derived 12-species mouse microbiota (Oligo-MM<sup>12</sup>) consisting of the following bacterial species: *Acutalibacter muris* sp. nov. KB18 (DSM 26090), *Flavonifractor plautii* YL31 (DSM 26117), *Clostridium clostridioforme* YL32 (DSM 26114), *Blautia coccoides* YL58 (DSM 26115), *Clostridium innocuum* I46 (DSM 26113), *Lactobacillus reuteri* I49 (DSM 32035), *Enterococcus faecalis* KB1 (DSM 32036), *Bacteroides caecimuris* sp. nov. I48 (DSM 26085), *Muribaculum intestinale* sp. nov. YL27 (DSM 28989), *Bifidobacterium longum* subsp. *animalis* YL2 (DSM 26074), *Turicimonas muris* sp. nov. YL45 (DSM 26109) and *Akkermansia muciniphila* YL44 (DSM 26127). A detailed description of the Oligo-MM<sup>12</sup> consortium species and description of novel taxa are provided by Brugioux *et al.*, (2016)<sup>38</sup> and Lagkouvardos *et al.*, (2016).<sup>62</sup> A group of seven sDMDMm2 mice (6–12 week old males) was used for the experiment. Gnotobiotic sDMDMm2 mice (Brugioux *et al.*, 2016) were established and maintained at the Clean Mouse Facility (CMF) of the Department of Clinical Research of the University of Bern. All animal experiments were performed in accordance with the Swiss Federal and the Bernese Cantonal regulations and were approved by the Bernese Cantonal ethical committee for animal experiments under license number BE 82/13.

### Bacterial strains and culture conditions

*Clostridium scindens* ATCC 35704 (Morris *et al.*, 1985)<sup>23</sup> was grown in BHIS-S medium, which contains 37g brain heart infusion (BHI), 5 g yeast extract, 40 mL salts solution (0.2 g CaCl<sub>2</sub>, 0.2 g MgSO<sub>4</sub>, 1 g K<sub>2</sub>HPO<sub>4</sub>, 1g KH<sub>2</sub>PO<sub>4</sub>, 10g NaHCO<sub>3</sub>, and 2g NaCl in 1 L ddH<sub>2</sub>O), 1g L-cysteine and 2



g fructose per L ddH<sub>2</sub>O or on BHIS-S agar (BHIS-S + 15g/L agar). The *in vitro* experiments were conducted in an anaerobic chamber (Coy Laboratory Products, 95% N<sub>2</sub>, 5% H<sub>2</sub>) at 37°C. For the *in vivo* experiments, erythromycin (10 µg/mL) was added to BHIS-S agar in order to select for *C. scindens* ATCC 35704 from mice intestinal content samples for quantification purposes. The selective plates (BHIS-S + erythromycin) were incubated in an anaerobic chamber (Don Whitley A45 HEPA, 10% CO<sub>2</sub>, 10% H<sub>2</sub>, 80% N<sub>2</sub>) for 72 h at 37°C.

### Impact of bile acids on bacterial growth

We assessed the impact of human (CA and CDCA) and murine (αMCA, βMCA, UDCA) primary and secondary (3-oxoDCA, 12-oxoLCA, DCA) bile acids on *C. scindens* growth *in vitro*. Cholic acid (CA, ref. A11257) was purchased from VWR, ursodeoxycholic acid (UDCA, ref. U5127) from Sigma-Aldrich, chenodeoxycholic acid (CDCA, ref. C0940-000), alpha-muricholic acid (αMCA, ref. C1890-000), beta-muricholic acid (βMCA, ref. C1895-000), deoxycholic acid (DCA, ref. C1070-000), 3-oxodeoxycholic acid (3-oxoDCA, ref. C1725-000) and 12-oxolithocholic acid (12-oxoLCA, ref. C1650-000) from Steraloids. These bile acids were dissolved in 100% ethanol and then, added to Erlenmeyer flasks with autoclaved and anoxic 150mL BHIS-S liquid medium (final concentration of ethanol in the medium ≤ 1%) to a final concentration of 100 µM. The concentration of 100 µM was chosen based on other studies investigating bile acid transformations *in vitro* but also to ensure the detection of minor transformation products.<sup>31,49</sup> An additional condition (CDCA at a concentration of 200 µM) was included as this concentration was also used for the bile acid transformation experiments *in vitro*. A control without bile acid (but with the ethanol vehicle) and a sterile control were prepared in parallel. For each bile acid condition or the controls, cultures were prepared in triplicate. Samples were taken regularly and OD<sub>600</sub> was immediately measured with a V-1200 spectrophotometer (VWR).

### Bile acid transformations experiments

Bile acid containing media and the controls (without bile acid) were inoculated with *C. scindens* to an initial OD<sub>600</sub> value of 0.050. Bile acids were probed at a concentration of 100 µM albeit a higher concentration was used for CDCA (200 µM) because of the low conversion to LCA and the attendant detection issues. This experiment was done in triplicates. A sterile control and an additional control without bile acid (but with the ethanol vehicle) were prepared in triplicates.

The tubes were incubated in an anaerobic chamber (Coy Laboratory Products, 95% N<sub>2</sub>, 5% H<sub>2</sub>) at 37°C. Samples were collected periodically and OD<sub>600</sub> was measured immediately after sampling. Each sample (1 mL) was centrifuged at 4°C for 5 minutes at 16,000 x g. The supernatant (SUP) was separated from the pellet (PEL) and placed in a new epitube. For experiments with DCA, 12-oxoLCA and 3-oxoDCA, an additional 1 mL of culture was collected. This sample containing both supernatant and biomass was named 'Total' (TOT). Samples (pellets, supernatants, total) were stored at -20°C to await bile acid analysis.

An additional experiment was conducted on a few PEL samples to determine whether the bile acids present in the pellet (biomass) are located intracellularly (in the cytoplasm) or are bound to the cell envelope. The selected pellets (CA t = 68 h, CDCA t = 44 h) were re-suspended in sterile water containing lysozyme (1 mg/mL) and incubated for 1 h at 37°C. After cell lysis, samples were ultracentrifuged (20,000 x g) at 4°C, for 30 min. The supernatant (corresponding to the cytoplasmic fraction) was collected in another epitube. The pellet (representing the cell envelope fraction) was also retained. All samples were stored at -20°C to await bile acid analysis.

### Cell-free extract (CFE) experiment

This experiment was designed to test whether the lack of intracellular transport of bile acids was responsible for the limited transformation of 3-oxoDCA and DCA by *C. scindens*. As a positive control, we also included 12-oxoLCA. This experiment was performed under anaerobic conditions, as bile acid 7-dehydroxylation is sensitive to oxygen.<sup>19</sup>



*C. scindens* was grown in BHIS-S medium. When bacterial growth reached mid-exponential phase ( $OD_{600} = 0.7$ ), CA was added to the culture to a final concentration of 100  $\mu\text{M}$ , in order to induce the synthesis of bile acid inducible (bai) enzymes. After 90 min of incubation with CA, the culture was centrifuged and the supernatant (containing CA) removed. The pellets of *C. scindens* cells were re-suspended in BHIS-S containing 2 mg/mL lysozyme and incubated at 37°C for 90 min. After cell lysis, 3-oxoDCA, DCA, or 12-oxoLCA were added separately to the medium ( $C_f = 100 \mu\text{M}$ ). This experiment was done in triplicates and samples were collected every 2 h during 10 h. Samples were stored at -20°C to await bile acid analysis.

### Preparation of standard solutions

Stock solutions [10 mM] of each internal and external BA standard were prepared in methanol. Deuterated LCA, DCA, CDCA, CA, TUDCA and TCA (Table S2) were used as internal standards (ISTD). Individual standard solutions [100  $\mu\text{M}$ ] were mixed together and diluted with ammonium acetate [5 mM] – methanol (50:50, v/v) to construct external standard curves between 1 and 10,000 nM. Each calibration level was spiked with the mixed ISTD solution [4  $\mu\text{M}$ ] for a final concentration of 500 nM. Additionally, 50  $\mu\text{L}$  of BHIS-S medium was added to each calibration level of the standard curves used for quantification of *in vitro* supernatant samples (SUP) to account for matrix effects.

### Bile acid extraction from cell cultures

Supernatants (SUP) from *in vitro* experiments were spiked with the mixed ISTD solution [4  $\mu\text{M}$ ] and diluted with ammonium acetate [5 mM] – methanol (50:50, v/v) to obtain the same final concentration of ISTD [500 nM].

BAs contained in pellets (PEL), in total (TOT) and cell-free extract (CFE) samples were extracted with the following protocol. Freeze-dried samples were first spiked with 100  $\mu\text{L}$  of mixed ISTD solution [100  $\mu\text{M}$ ] and then extracted with 500  $\mu\text{L}$  of ice-cold alkaline acetonitrile in 2 mL tubes filled with 0.5 mm glass beads using an automated Precellys 24 Tissue Homogenizer (Bertin Instruments) at 6,500 rpm for 3  $\times$  30 s with a 30 s break. Samples

were vigorously vortexed, and continuously shaken for 1 h at room temperature. The mixtures were centrifuged at 16,000  $\times$  g for 10 min and the supernatants collected and lyophilized in a rotational vacuum concentrator (Christ) before reconstitution in 1 mL of ammonium acetate [5 mM] – methanol (50:50, v/v) pH 6. The reconstituted samples were further diluted 20 times in the same solution prior to LC-MS injection.

### Isotopic labeling of *C. scindens* cells

*C. scindens* was serially grown ( $\geq 50$  generations) in medium composed of a 9:1 ratio of Celtone Complete Medium (CCM –  $^{13}\text{C}$ , 98%+,  $^{15}\text{N}$ , 98%+) to BHIS-S<sub>1/2</sub> medium. BHIS-S<sub>1/2</sub> corresponds to a 1:1 mixture of BHIS-S medium and sterile ddH<sub>2</sub>O amended with 5 g/L of Celtone Base Powder (CBP –  $^{13}\text{C}$ , 98%+,  $^{15}\text{N}$ , 98%+). *C. scindens* did not grow in the CCM alone and required the amendment of a small volume of BHIS-S<sub>1/2</sub>. The final labeled medium contained only a small amount of unlabeled nutrients (coming from BHIS-S).

An unlabeled culture of *C. scindens* (control) was prepared following the same protocol but with unlabeled CCM and unlabeled CBP. Labeled CCM (ref. CGM-1040-CN-0.1) and CBP (ref. CGM-1030P-CN-PK), as well as unlabeled CCM (ref. CGM-1040-U-0.1) and CBP (ref. CGM-1030P-U-PK) were purchased from Cambridge Isotope Laboratories.

### In vitro experiment: dilution of *C. scindens* isotopic labeling in unlabeled medium

*C. scindens* was labeled *in vitro* according to the procedure described above. The labeled cells were transferred into BHIS-S medium (lacking labeled nutrient) and incubated anaerobically at 37°C for 24 h while sampling periodically. Growth was quantified using  $OD_{600}$  measurement. All the samples were fixed in 2.5% glutaraldehyde and rinsed at least three times with sterile ddH<sub>2</sub>O. Samples were stored at 4°C to await NanoSIMS analysis.

### Animal experiment

Cultures of isotopically labeled and unlabeled (control) *C. scindens* were centrifuged and washed in

PBS-1X prior to mouse gavage. A total of seven sDMDMm2 mice were included in our study. Four mice were inoculated with  $10^9$  labeled *C. scindens* cells (L-mice) and two mice with  $10^9$  unlabeled *C. scindens* cells (U-mice). A sample of the inoculum was kept for NanoSIMS analysis. One additional mouse was used as a control and was gavaged only with PBS-1X. Only for bile acid analysis, two additional control mice were included in the study to have an equal number of mice in the two groups compared (Figures 6, 7 and 8). Six and twenty-four hours after inoculation, 2 ‘L-mice’ and 1 ‘U-mice’ were sacrificed. The control mouse was sacrificed at the end of the experiment ( $t_{24h}$ ). The content of four intestinal compartments were collected: two parts of the small intestine (jejunum and ileum), the cecum and the colon. For each sample, the intestinal content was divided into 3 tubes for the different analyses. The samples for NanoSIMS (intestinal contents samples and *C. scindens* inoculum) were fixed with 2.5% glutaraldehyde (for a minimum of 3 h). The fixed samples were rinsed (at least 3 times) with sterile ddH<sub>2</sub>O and stored at 4°C to await NanoSIMS analysis. The samples for bile acid analysis were stored at –20°C. The samples for *C. scindens* quantification were directly plated on a selective medium (BHIS-S + erythromycin) and incubated in an anoxic chamber at 37° for 72 h. In the results part, *C. scindens* counts are expressed as colony-forming unit (CFU) per gram of fecal content. The values indicated in the paper represent the mean  $\pm$  standard deviation.

### Nanosims sample preparation and analysis

Two types of samples were analyzed by NanoSIMS: the *in vitro* samples (*C. scindens* culture), and the *in vivo* samples (mouse intestinal contents). Regarding the *in vivo* experiment, samples of one L-mouse per time point were chosen for the analysis.

The fixed samples (from the *in vitro* and *in vivo* experiments) were mounted on silicon wafers: for each sample, 5 to 10  $\mu$ L of bacterial suspension was deposited in the center of the silicon wafers and dried at 37°C. The silicon wafers were then coated with 10 nm of gold to avoid charging effects. The distribution of the secondary ions species  $^{12}\text{C}^{15}\text{N}^-$ ,  $^{12}\text{C}^{14}\text{N}^-$ ,  $^{12}\text{C}^{13}\text{C}^-$ , and  $^{12}\text{C}^{12}\text{C}^-$  on bacterial cells was mapped with a NanoSIMS 50L (Cameca)

operating at a mass resolution of  $> 9000$  (Cameca definition), sufficient to resolve these masses from potential mass interferences. Images of typically  $30 \times 30 \mu\text{m}^2$  with a resolution of  $256 \times 256$  pixels and a primary beam diameter of about 120 nm were collected across the samples. Each NanoSIMS image consists of 5 sequential images that were drift corrected, and accumulated using the software L’IMAGE (developed by Dr. Larry Nittler, Carnegie Institution of Washington, USA). Nitrogen and carbon isotopes ratio images were obtained by taking the ratio between the cumulated  $^{12}\text{C}^{15}\text{N}^-$ ,  $^{12}\text{C}^{14}\text{N}^-$  and  $^{12}\text{C}^{13}\text{C}^-$ ,  $^{12}\text{C}^{12}\text{C}^-$  images, and reported in the delta notation against a control sample of normal isotopic composition measured several times during the same run:

$$R(\text{in } \%) = \left( \frac{R_{\text{Sample}}}{R_{\text{Control}}} - 1 \right) \times 1000, \text{ where } R$$

represents either  $^{15}\text{N}/^{14}\text{N}$  or  $^{13}\text{C}/^{12}\text{C}$ , respectively.

Regions of interest (ROIs) were drawn around single *C. scindens* cells or small cluster of cells with the software L’IMAGE to quantify mean  $\delta^{15}\text{N}$  enrichments of the *C. scindens* cells along the intestinal tract or in BHIS-S medium (for the *in vitro* experiment).

### Bile acid extraction from intestinal content

Approximately 10 milligrams of freeze-dried intestinal contents were homogenized with 200  $\mu$ L of ISTD solution ([1mM or 25 $\mu$ M] depending on the intestinal compartment) in 2 mL tubes filled with 2.8 mm zirconium oxide beads. Homogenization was performed using an automated Precellys 24 Tissue Homogenizer (Bertin Instruments) at 5000 rpm for  $1 \times 20$  s. Mixed samples were equilibrated on ice for 1 h. An amount of 500  $\mu$ L of ice-cold alkaline acetonitrile (5% ammonia in acetonitrile) was added to the homogenates, which were then vigorously vortexed, and continuously shaken for 1 h at room temperature. The mixtures were centrifuged at  $16,000 \times g$  for 10 min and the supernatants collected. The pellets were extracted with another 500  $\mu$ L of ice-cold alkaline acetonitrile. Supernatants from the two extractions steps were pooled and lyophilized in a rotational vacuum concentrator (Christ) before reconstitution in 100  $\mu$ L of ammonium acetate (5 mM) – methanol (50:50, v/v) pH 6 and stored at –20°C. Supernatants were diluted according to the intestinal compartment (4000 times

for the small intestine samples and 100 times for the cecum and colon samples) for LC-MS injection.

### UHPLC-HRMS analyses

Both qualitative and quantitative analyses were conducted on an Agilent 6530 Accurate-Mass Q-TOF LC/MS mass spectrometer coupled to an Agilent 1290 series UHPLC system (Agilent Technologies). The separation was achieved using a Zorbax Eclipse-Plus C18 column (2.1 × 100 mm, 1.8 µm; Agilent Technologies) heated at 50°C. A binary gradient system consisted of ammonium acetate [5 mM] pH 6 in water as eluent A and acetonitrile as eluent B. The sample separation was carried out at 0.4 mL/min over a 22 min total run time using the following program: 0–5.5 min, isocratic 21.5% B; 5.5–6 min, 21.5–24.5% B; 6–10 min, 24.5–25% B; 10–10.5 min, 25–29% B; 10.5–14.5 min, isocratic 29% B; 14.5–15 min, 29–40% B; 15–18 min, 40–45% B; 18–20.5 min, 45–95% B, 20.5–22 min, isocratic 95%. The system was re-equilibrated in initial conditions for 3 min. The sample manager system temperature was maintained at 4°C and the injection volume was 5 µL. Mass spectrometer detection was operated in negative ionization mode using the Dual AJS Jet stream ESI Assembly. The QTOF instrument was operated in 4 GHz high-resolution mode (typical resolution 17,000 (FWHM) at  $m/z$  1000) in profile mode and calibrated in negative full scan mode using ESI-L solution (Agilent Technologies). Internal calibration was performed during acquisition via continuous infusion of a reference mass solution [5 mM purine, 1 mM HP-921 (Agilent reference mass kit, Agilent Technologies) in 95% MeOH acidified with 0.1% formic acid] and allowed to permanently achieve a mass accuracy better than 5 ppm. HR mass spectra were acquired over the range of  $m/z$  100–1700 at an acquisition rate of 5 spectra/s. AJS settings were as follows: drying gas flow, 8 L/min; drying gas temperature, 300°C; nebulizer pressure, 35 psi; capillary voltage, 3500 V; nozzle voltage, 1000 V; fragmentor voltage, 175 V; skimmer voltage, 65 V; octopole 1 RF voltage, 750 V. Data were processed using the MassHunter Workstation (Agilent Technologies). According to this method, 40 bile acids (SI Table 2) were quantified by external calibration curves and corrected with internal standards. Extracted ions

chromatograms (EIC) were based on a retention time (RT) window of  $\pm 0.5$  min with a mass-extraction-windows (MEW) of  $\pm 30$  ppm centered on  $m/z_{\text{theor}}$  of each bile acid. For each BA, the limits of detection (LODs) were estimated by using the signal-to-noise ratio (S/N) equal to or over 3, values calculated automatically by the program after injection of serially diluted calibration standard solutions (Table S2).

### Statistical analysis

All statistical analyses were performed using GraphPad Prism 7 software (GraphPad Software). The statistical tests used are indicated in the figure legends. P values < 0.05 were considered statistically significant.

### Disclosure of potential conflicts of interest

No potential conflicts of interest were disclosed.

### Funding

This work was supported by the Swiss National Science Foundation (grants #CRSII3\_147603 and #CRSII5\_180317).

### ORCID

Nicolas Studer  <http://orcid.org/0000-0002-6496-3303>  
Stéphane Escrig  <http://orcid.org/0000-0002-7525-4000>  
Anders Meibom  <http://orcid.org/0000-0002-4542-2819>  
Siegfried Hapfelmeier  <http://orcid.org/0000-0002-6913-7932>  
Rizlan Bernier-Latmani  <http://orcid.org/0000-0001-6547-722X>

### References

1. Hofmann AF. The continuing importance of bile acids in liver and intestinal disease. *Arch Intern Med.* 1999;159:2647–2658. doi:10.1001/archinte.159.22.2647.
2. Swann JR, Want EJ, Geier FM, Spagou K, Wilson ID, Sidaway JE, Nicholson JK, Holmes E. Systemic gut microbial modulation of bile acid metabolism in host tissue compartments. *Proc Natl Acad Sci.* 2011;108:4523–4530. doi:10.1073/pnas.1006734107.
3. Van Nierop FS, Scheltema MJ, Eggink HM, Pols TW, Sonne DP, Knop FK, Soeters MR. Clinical relevance of the bile acid receptor TGR5 in metabolism. *Lancet Diabetes Endocrinol.* 2017;5:224–233. doi:10.1016/S2213-8587(16)30155-3.

4. Kuipers F, Bloks VW, Groen AK. Beyond intestinal soap-bile acids in metabolic control. *Nat Rev Endocrinol*. 2014;10:488–498. doi:10.1038/nrendo.2014.60.
5. Wahlström A, Sayin SI, Marschall HU, Bäckhed F. Intestinal crosstalk between bile acids and microbiota and its impact on host metabolism. *Cell Metab*. 2016;24:41–50. doi:10.1016/j.cmet.2016.05.005.
6. Schaap FG, Trauner M, Jansen PLM. Bile acid receptors as targets for drug development. *Nat Rev Gastroenterol Hepatol*. 2013;11:1–13.
7. Buffie CG, Bucci V, Stein RR, McKenney PT, Ling L, Gobourne A, No D, Liu H, Kinnebrew M, Viale A, et al. Precision microbiome restoration of bile acid-mediated resistance to *Clostridium difficile*. *Nature*. 2015;517:205–208. doi:10.1038/nature13828.
8. Joyce SA, Gahan CGM. Bile acid modifications at the microbe-host interface: potential for nutraceutical and pharmaceutical interventions in host health. In: editors, Doyle MP, Klaenhammer TR. *Annu Rev Food Sci Technol*. 2016;7:313–333. doi: 10.1146/annurev-food-041715-033159.
9. Thomas C, Pellicciari R, Pruzanski M, Auwerx J, Schoonjans K. Targeting bile-acid signalling for metabolic diseases. *Nat Rev Drug Discov*. 2008;7:678–693. doi:10.1038/nrd2619.
10. Bernstein H, Bernstein C, Payne CM, Dvorakova K, Garewal H. Bile acids as carcinogens in human gastrointestinal cancers. *Mutat Res*. 2005;589:47–65. doi:10.1016/j.mrrev.2004.08.001.
11. Joyce SA, MacSharry J, Casey PG, Kinsella M, Murphy EF, Shanahan F, Hill C, Gahan CGM. Regulation of host weight gain and lipid metabolism by bacterial bile acid modification in the gut. *Proc Natl Acad Sci*. 2014;111:7421–7426. doi:10.1073/pnas.1323599111.
12. Tropini C, Earle KA, Huang KC, Sonnenburg JL. The gut microbiome: connecting spatial organization to function. *Cell Host Microbe*. 2017;21:433–442. doi:10.1016/j.chom.2017.03.010.
13. Donaldson GP, Lee SM, Mazmanian SK. Gut biogeography of the bacterial microbiota. *Nat Rev Microbiol*. 2015;14:20–32. doi:10.1038/nrmicro3552.
14. Midtvedt T, Norman A. Anaerobic, bile acid transforming microorganisms in rat intestinal content. *Acta Pathol Microbiol Scand*. 1968;72:337–344. doi:10.1111/j.1699-0463.1968.tb01347.x.
15. Sayin SI, Wahlström A, Felin J, Jäntti S, Marschall H-U, Bamberg K, Angelin B, Hyötyläinen T, Orešić M, Bäckhed F. Gut microbiota regulates bile acid metabolism by reducing the levels of tauro-beta-muricholic acid, a naturally occurring FXR antagonist. *Cell Metab*. 2013;17:225–235. doi:10.1016/j.cmet.2013.01.003.
16. Kitahara M, Takamine F, Imamura T, Benno Y. *Clostridium hiranonis* sp. nov., a human intestinal bacterium with bile acid 7 $\alpha$ -dehydroxylating activity. *Int J Syst Evol Microbiol*. 2001;51:39–44. doi:10.1099/00207713-51-1-39.
17. Narushima S, Itoh K, Takamine F, Uchida K. Absence of cecal secondary bile acids in gnotobiotic mice associated with two human intestinal bacteria with the ability to dehydroxylate bile acids in vitro. *Microbiol Immunol*. 1999;43:893–897.
18. Batta AK, Salen G, Arora R, Shefer S, Batta M, Person A. Side chain conjugation prevents bacterial 7-dehydroxylation of bile acids. *J Biol Chem*. 1990;265:10925–10928.
19. Stellwag EJ, Hylemon PB. 7 $\alpha$ -Dehydroxylation of cholic acid and chenodeoxycholic acid by *Clostridium leptum*. *J Lipid Res*. 1979;20:325–333.
20. Masuda N, Oda H, Hirano S, Hiromitsu A. Enhancement of the 7 $\alpha$ -dehydroxylase activity of a gram-positive intestinal anaerobe by flavins. *Appl Environ Microbiol*. 1983;45:308–309.
21. Hirano S, Masuda N. Enhancement of the 7 $\alpha$ -dehydroxylase activity of a gram-positive intestinal anaerobe by *Bacteroides* and its significance in the 7-dehydroxylation of ursodeoxycholic acid. *J Lipid Res*. 1982;23:1152–1158.
22. Eyssen HJ, De Pauw G, Van Eldere J. Formation of hyodeoxycholic acid from muricholic acid and hyocholic acid by an unidentified gram-positive rod termed HDCA-1 isolated from rat intestinal microflora. *Appl Environ Microbiol*. 1999;65:3158–3163.
23. Morris GN, Winter J, Cato EP, Ritchie AE, Bokkenheuser VD. *Clostridium scindens* sp. nov., a human intestinal bacterium with desmolytic activity on corticoids. *Int J Syst Bacteriol*. 1985;35:478–481. doi:10.1099/00207713-35-4-478.
24. Kitahara M, Takamine F, Imamura T, Benno Y. Assignment of *Eubacterium* sp. VPI 12708 and related strains with high bile acid 7 $\alpha$ -dehydroxylating activity to *Clostridium scindens* and proposal of *Clostridium hylemonae* sp. nov., isolated from human faeces. *Int J Syst Evol Microbiol*. 2000;50:971–978. doi:10.1099/00207713-50-3-971.
25. Tawthep S, Fukiya S, Lee J-Y, Hagio M, Ogura Y, Hayashi T, Yokota A. Isolation of six novel 7-oxo- or urso-type secondary bile acid-producing bacteria from rat cecal contents. *J Biosci Bioeng*. 2017;124:514–522. doi:10.1016/j.jbiosc.2017.06.002.
26. White BA, Lipsky RL, Fricke RJ, Hylemon PB. Bile acid induction specificity of 7 $\alpha$ -dehydroxylase activity in an intestinal *Eubacterium* species. *Steroids*. 1980;35:103–109. doi:10.1016/0039-128X(80)90115-4.
27. Shen A, Miller VL. A gut odyssey: the impact of the microbiota on *Clostridium difficile* spore formation and germination. *PLoS Pathog*. 2015;11:e1005157. doi:10.1371/journal.ppat.1005157.
28. Greathouse KL, Harris CC, Bultman SJ. Dysfunctional families: *Clostridium scindens* and secondary bile acids inhibit the growth of *Clostridium difficile*. *Cell Metab*. 2015;21:9–10. doi:10.1016/j.cmet.2014.12.016.
29. Hoppe P, Cohen S, Meibom A. GGR cutting-edge review nanosims: technical aspects and applications in



- cosmochemistry and biological geochemistry. *Geostand Geoanal Res.* 2013;37:111–154. doi:[10.1111/j.1751-908X.2013.00239.x](https://doi.org/10.1111/j.1751-908X.2013.00239.x).
30. Macdonald IA, Hutchison DM. Epimerization versus dehydroxylation of the 7 $\alpha$ -hydroxyl- group of primary bile acids: competitive studies with *Clostridium* absolum and 7 $\alpha$ -dehydroxylating bacteria (*Eubacterium* SP.). *J Steroid Biochem.* 1982;17:287–293. doi:[10.1016/0022-4731\(82\)90203-5](https://doi.org/10.1016/0022-4731(82)90203-5).
  31. Takamine F, Imamura T. Isolation and characterization of bile acid 7-dehydroxylating bacteria from human feces. *Microbiol Immunol.* 1995;39:11–18. doi:[10.1111/j.1348-0421.1995.tb02162.x](https://doi.org/10.1111/j.1348-0421.1995.tb02162.x).
  32. Ridlon JM, Harris SC, Bhowmik S, Kang D-J-J, Hylemon PB. Consequences of bile salt biotransformations by intestinal bacteria. *Gut Microbes.* 2016;7:22–39. doi:[10.1080/19490976.2015.1127483](https://doi.org/10.1080/19490976.2015.1127483).
  33. Kollerov VV, Lobastova TG, Monti D, Deshcherevskaya NO, Ferrandi EE, Fronza G, Riva S, Donova MV. Deoxycholic acid transformations catalyzed by selected filamentous fungi. *Steroids.* 2016;107:20–29. doi:[10.1016/j.steroids.2015.12.015](https://doi.org/10.1016/j.steroids.2015.12.015).
  34. Zhang Y, Klaassen CD. Effects of feeding bile acids and a bile acid sequestrant on hepatic bile acid composition in mice. *J Lipid Res.* 2010;51:3230–3242. doi:[10.1194/jlr.M007641](https://doi.org/10.1194/jlr.M007641).
  35. Hirano S, Masuda N. Transformation of bile acids by *Eubacterium lentum*. *Appl Environ Microbiol.* 1981;42:912–915.
  36. Hirano S, Masuda N, Oda H, Imamura T. Transformation of bile acids by mixed microbial cultures from human feces and bile acid transforming activities of isolated bacterial strains. *Microbiol Immunol.* 1981;25:271–282. doi:[10.1111/j.1348-0421.1981.tb00029.x](https://doi.org/10.1111/j.1348-0421.1981.tb00029.x).
  37. Wells JE, Hylemon PB. Identification and characterization of a bile acid 7 $\alpha$ -dehydroxylation operon in *Clostridium* sp. strain TO-931, a highly active 7 $\alpha$ -dehydroxylating strain isolated from human feces. *Appl Environ Microbiol.* 2000;66:1107–1113. doi:[10.1128/AEM.66.3.1107-1113.2000](https://doi.org/10.1128/AEM.66.3.1107-1113.2000).
  38. Brugioux S, Beutler M, Pfann C, Garzetti D, Ruscheweyh H-J, Ring D, Diehl M, Herp S, Lötscher Y, Hussain S, et al. Genome-guided design of a defined mouse microbiota that confers colonization resistance against *Salmonella enterica* serovar Typhimurium. *Nat Microbiol.* 2016;2:16215. doi:[10.1038/nmicrobiol.2016.215](https://doi.org/10.1038/nmicrobiol.2016.215).
  39. Studer N, Desharnais L, Beutler M, Brugioux S, Terrazos MA, Menin L, Schürch CM, McCoy KD, Kuehne SA, Minton NP, et al. Functional intestinal bile acid 7 $\alpha$ -Dehydroxylation by *Clostridium scindens* associated with protection from *clostridium difficile* infection in a gnotobiotic mouse model. *Front Cell Infect Microbiol.* 2016;6:191. doi:[10.3389/fcimb.2016.00191](https://doi.org/10.3389/fcimb.2016.00191).
  40. Hofmann AF, Eckmann L. How bile acids confer gut mucosal protection against bacteria. *Proc Natl Acad Sci.* 2006;103:4333–4334. doi:[10.1073/pnas.0600780103](https://doi.org/10.1073/pnas.0600780103).
  41. Islam KBMS, Fukiya S, Hagio M, Fujii N, Ishizuka S, Ooka T, Ogura Y, Hayashi T, Yokota A. Bile acid is a host factor that regulates the composition of the cecal microbiota in rats. *Gastroenterol.* 2011;141:1773–1781. doi:[10.1053/j.gastro.2011.07.046](https://doi.org/10.1053/j.gastro.2011.07.046).
  42. Inagaki T, Moschetta A, Lee Y-K, Peng L, Zhao G, Downes M, Yu RT, Shelton JM, Richardson JA, Repa JJ, et al. Regulation of antibacterial defense in the small intestine by the nuclear bile acid receptor. *Proc Natl Acad Sci.* 2006;103:3920–3925. doi:[10.1073/pnas.0509592103](https://doi.org/10.1073/pnas.0509592103).
  43. Shapiro H, Kolodziejczyk AA, Halstuch D, Elinav E. Bile acids in glucose metabolism in health and disease. *J Exp Med.* 2018;2017:1965. doi:[10.1084/jem.20171965](https://doi.org/10.1084/jem.20171965).
  44. Yoshimoto S, Loo TM, Atarashi K, Kanda H, Sato S, Oyadomari S, Iwakura Y, Oshima K, Morita H, Hattori M, et al. Obesity-induced gut microbial metabolite promotes liver cancer through senescence secretome. *Nature.* 2013;499:97–101. doi:[10.1038/nature12347](https://doi.org/10.1038/nature12347).
  45. Sacquet EC, Gadelle DP, Riottot MJ, Raibaud APM. Absence of transformation of  $\beta$ -Muricholic acid by human microflora implanted in the digestive tracts of germfree male rats. *Appl Environ Microbiol.* 1984;47:1167–1168.
  46. White BA, Fricke RJ, Hylemon PB. 7 beta-Dehydroxylation of ursodeoxycholic acid by whole cells and cell extracts of the intestinal anaerobic bacterium, *Eubacterium* species V.P.I. 12708. *J Lipid Res.* 1982;23:145–153.
  47. Ridlon JM, Kang DJ, Hylemon PB. Isolation and characterization of a bile acid inducible 7 $\alpha$ -dehydroxylating operon in *Clostridium hylemonae* TN271. *Anaerobe.* 2010;16:137–146. doi:[10.1016/j.anaerobe.2009.07.006](https://doi.org/10.1016/j.anaerobe.2009.07.006).
  48. Winter J, Gn M, O'Rourke-Locascio S, Vd B, Eh M, Bi C, Pb H. Mode of action of steroid desmolase and reductases synthesized by *Clostridium 'scindens'* (formerly *Clostridium* strain 19). *J Lipid Res.* 1984;25:1124–1131.
  49. Hirano S, Nakama R, Tamaki M, Masuda N, Oda H. Isolation and characterization of thirteen intestinal microorganisms capable of 7 $\alpha$ -dehydroxylating bile acids. *Appl Environ Microbiol.* 1981;41:737–745.
  50. Bhowmik S, Jones DH, Chiu H-P, Park I-H, Chiu H-J, Axelrod HL, Farr CL, Tien HJ, Agarwalla S, Lesley SA. Structural and functional characterization of BaiA, an enzyme involved in secondary bile acid synthesis in human gut microbe. *Proteins.* 2014;82:216–229. doi:[10.1002/prot.24353](https://doi.org/10.1002/prot.24353).
  51. Harris SC, Devendran S, Alves JMP, Mythen SM, Hylemon PB, Ridlon JM, Bhowmik S, Jones DH, Chiu H-P, Park I-H, et al. Identification of a gene encoding a flavoprotein involved in bile acid metabolism by the human gut bacterium *Clostridium scindens* ATCC



35704. *Biochim Biophys Acta - Mol Cell Biol Lipids*. 2018;1863:276–283. doi:[10.1016/j.bbalip.2017.12.001](https://doi.org/10.1016/j.bbalip.2017.12.001).
52. Doden H, Sallam LA, Devendran S, Ly L, Doden G, Daniel SL, Alves JMP, Ridlon JM, Müller V. Metabolism of oxo-bile acids and characterization of recombinant 12 $\alpha$ -hydroxysteroid dehydrogenases from bile acid 7 $\alpha$ -dehydroxylating human gut bacteria *Clostridium scindens* ATCC 35704, *Clostridium hylemonae* DSM 15053 and *Clostridium hiranonis* DSM 13275. *Appl Environ Microbiol*. 2018;84: doi:[10.1128/AEM.00235-18](https://doi.org/10.1128/AEM.00235-18).
  53. Midtvedt T, Norman A. Parameters in 7 $\alpha$ -dehydroxylation of bile acids by anaerobic lactobacilli. *Acta Pathol Microbiol Scand*. 1968;72:313–329. doi:[10.1111/j.1699-0463.1968.tb01345.x](https://doi.org/10.1111/j.1699-0463.1968.tb01345.x).
  54. Gerard P, Gérard P. Metabolism of cholesterol and bile acids by the gut microbiota. *Pathogens*. 2013;3:14–24. doi:[10.3390/pathogens3010014](https://doi.org/10.3390/pathogens3010014).
  55. Ridlon JM, Kang D-J, Hylemon PB. Bile salt biotransformations by human intestinal bacteria. *J Lipid Res*. 2006;47:241–259. doi:[10.1194/jlr.M600040-JLR200](https://doi.org/10.1194/jlr.M600040-JLR200).
  56. Devlin AS, Fischbach MA. A biosynthetic pathway for a prominent class of microbiota-derived bile acids. *Nat Chem Biol*. 2015;11:685–690. doi:[10.1038/nchembio.1864](https://doi.org/10.1038/nchembio.1864).
  57. Musat N, Musat F, Weber PK, Pett-Ridge J. Tracking microbial interactions with NanoSIMS. *Curr Opin Biotechnol*. 2016;41:114–121. doi: [10.1016/j.copbio.2016.06.007](https://doi.org/10.1016/j.copbio.2016.06.007).
  58. Neufeld JD, Wagner M, Murrell JC. Who eats what, where and when? Isotope-labelling experiments are coming of age. *ISME J*. 2007;1:103–110. doi:[10.1038/ismej.2007.39](https://doi.org/10.1038/ismej.2007.39).
  59. Gibbin E, Gavish A, Domart-Coulon I, Kramarsky-Winter E, Shapiro O, Meibom A, Vardi A. Using NanoSIMS coupled with microfluidics to visualize the early stages of coral infection by *Vibrio coralliilyticus*. *BMC Microbiol*. 2018;18:39. doi:[10.1186/s12866-018-1202-z](https://doi.org/10.1186/s12866-018-1202-z).
  60. Alnouti Y. Bile acid sulfation: a pathway of bile acid elimination and detoxification. *Toxicol Sci*. 2009;108:225–246. doi:[10.1093/toxsci/kfn268](https://doi.org/10.1093/toxsci/kfn268).
  61. Pacini N, Albini E, Ferrari A, Zanchi R, Marca G, Bandiera T. Transformation of sulfated bile acids by human intestinal microflora. *Arzneimittelforschung*. 1987;37:983–987.
  62. Lagkouvardos I, Pukall R, Abt B, Foesel BU, Meier-Kolthoff JP, Kumar N, Bresciani A, Martínez I, Just S, Ziegler C, et al. The Mouse Intestinal Bacterial Collection (miBC) provides host-specific insight into cultured diversity and functional potential of the gut microbiota. *Nat Microbiol*. 2016;1:16131. doi:[10.1038/nmicrobiol.2016.131](https://doi.org/10.1038/nmicrobiol.2016.131).